NACA RM L9L06

NACA

RESEARCH MEMORANDUM

SPIN-TUNNEL INVESTIGATION OF A MODEL OF A 60° DELTA-WING AIRPLANE TO DETERMINE THE SPIN, RECOVERY, AND LONGITUDINAL TRIM CHARACTERISTICS THROUGHOUT AN EXTENSIVE RANGE OF MASS LOADINGS

By Walter J. Klinar and Ira P. Jones, Jr.

Langley Aeronautical Laboratory
Langley Air Force Base, Va.

NATIONAL ADVISORY COMMITTEE
FOR AERONAUTICS

WASHINGTON
February 15, 1950

NATIONAL ADVISORY COMMITTEE FOR AERONAUTICS

RESEARCH MEMORANDUM

SPIN-TUNNEL INVESTIGATION OF A MODEL OF A 60° DELTA-WING AIRPLANE TO DETERMINE THE SPIN, RECOVERY, AND LONGITUDINAL TRIM CHARACTERISTICS THROUGHOUT AN EXTENSIVE RANGE OF MASS LOADINGS

By Walter J. Klinar and Ira P. Jones, Jr.

SUMMARY

An investigation has been conducted in the Langley 20-foot free-spinning tunnel to determine the spin, recovery, and longitudinal-trim characteristics of a 60° delta-wing model throughout an extensive range of mass loadings. The spin investigation included variations in the relative density, center-of-gravity position, and inertia parameters. Glide tests and static force tests were performed to determine whether any unusual trimming tendencies above the stall were likely to exist for designs of this type.

The investigation showed that with a single-vertical-tail configuration, the model did not spin for a wide range of values of the inertia yawing-moment parameter. As the inertia yawing-moment parameter was increased or decreased from this range of values, however, spins were obtained. The results showed that, although reversal of the rudder on the single-vertical-tail configuration was generally ineffective in terminating the spin rotation, movement of the ailerons to full with the spin was very effective. When either of two large-dual-vertical-tail arrangements were installed, reversal of the rudders also stopped the spin rotation.

The results of the glide tests and the static force tests indicated that trim conditions above the stall would generally be obtained when the elevators were full up but that trim attitudes above the stall with the elevators at neutral or down probably would not be obtained unless the center of gravity was relatively far rearward.

INTRODUCTION

Because of current interest in delta-wing aircraft, an investigation was undertaken in the Langley 20-foot free-spinning tunnel to determine the spin and recovery characteristics throughout a wide range of mass loadings of a model of a jet-propelled airplane with no horizontal tail having a delta wing with a 60° apex angle. For the investigation, the relative density was varied from approximately 15 to 30, the center of gravity was varied from approximately 24 to 35 percent of the mean aerodynamic chord, and the inertia yawing-moment parameter was varied from approximately -70×10^{-4} to -1500×10^{-4}, the maximum variation obtainable on the model. The basic model configuration had a single vertical tail mounted at the center of the fuselage, but several dual-vertical-tail configurations were also investigated.

In addition to the spin investigation, force tests were conducted from 0° to 90° angle of attack, and tests with the model in free gliding flight in the tunnel were also performed to determine the longitudinal trim characteristics of the model. The force tests were conducted on the model used for the spin and glide tests and also on a larger model.

SYMBOLS

b	wing span, feet
S	wing area, square feet
$\bar{c}$	mean aerodynamic chord, feet
$x/\bar{c}$	ratio of distance of center of gravity rearward of leading edge of mean aerodynamic chord to mean aerodynamic chord
$z/\bar{c}$	ratio of distance between center of gravity and fuselage reference line to mean aerodynamic chord (positive when center of gravity is below fuselage reference line)
m	mass of airplane, slugs
I_X, I_Y, I_Z	moments of inertia about X, Y, and Z body axes, respectively, slug-feet^2
$\frac{I_X - I_Y}{mb^2}$	inertia yawing-moment parameter

$\frac{I_Y - I_Z}{mb^2}$	inertia rolling-moment parameter
$\frac{I_Z - I_X}{mb^2}$	inertia pitching-moment parameter
ρ	air density, slug per cubic foot
μ	relative density of airplane $\left(\frac{m}{\rho S b}\right)$
R	Reynolds number
α	angle of attack, degrees (For the spin data presented on the charts, α is the angle between fuselage reference line and vertical and is approximately equal to the absolute value of the angle of attack at plane of symmetry.)
ϕ	angle between span axis and horizontal, degrees
V	full-scale true rate of descent, feet per second
Ω	full-scale angular velocity about spin axis, revolutions per second
L	lift, pounds
D	drag, pounds
M	pitching moment about center of gravity of airplane, foot-pounds
q	dynamic pressure, pounds per square foot
C_L	lift coefficient (L/qS)
C_D	drag coefficient (D/qS)
C_m	pitching-moment coefficient ($M/qS\bar{c}$)
ψ	angle of yaw about Z body axis, degrees
δ_e	elevator deflection, positive when trailing edge is down, degrees

δ_a aileron deflection, degrees

δ_r rudder deflection, positive when trailing edge is to the left, degrees

APPARATUS AND METHODS

Models

The model used for the spin investigation and the glide tests was of such proportions as to be considered representative of a $\frac{1}{20}$-scale model of a fighter-type airplane, and the dimensional characteristics of a corresponding full-scale airplane are given in table I. Figure 1 is a three-view drawing of the $\frac{1}{20}$-scale model, and the various dual-vertical-tail arrangements tested on the model are shown in figure 2. Comparison of figure 1 and figure 2 shows that the wing span of the model was reduced somewhat when the dual vertical tails were installed. A photograph of the $\frac{1}{20}$-scale model spinning in the tunnel is shown as figure 3. The larger model, which was used only for force tests, was considered to be a $\frac{1}{12}$-scale representation of the airplane and is shown mounted in the tunnel in figure 4.

For the models used for this investigation, lateral and longitudinal control were combined in one pair of surfaces called elevons. Longitudinal control was obtained by deflecting the elevons together, and lateral control by differential deflection of the elevons. Hereinafter, elevon deflections for longitudinal and lateral control will be referred to, for simplicity, as elevator deflection and aileron deflection, respectively.

The $\frac{1}{20}$-scale model was ballasted with lead weights to obtain dynamic similarity to a corresponding airplane at an altitude of 15,000 feet (ρ = 0.001496 slug/cu ft). The weight, moments of inertia, and center-of-gravity location used in ballasting the model were selected on the basis of dimensions of an airplane typical of this type.

A remote-control mechanism was installed in the model to actuate the controls for recovery. Sufficient moments were exerted on the control surfaces during recovery attempts to move them fully and rapidly

Wind Tunnel and Testing Technique

The tests were performed in the Langley 20-foot free-spinning tunnel, the operation of which is generally similar to that described in reference 1 for the Langley 15-foot free-spinning tunnel.

Spin tests.- The model-launching technique for spin tests has been changed from that described in reference 1 in that the model is now launched by hand with rotation into the vertically rising air stream. After a number of turns in the established spin, a recovery attempt is made by moving one or more controls by means of the remote-control mechanism. The spin data obtained from these tests are then converted to corresponding full-scale values by methods described in reference 1.

In accordance with standard spin-tunnel procedure, tests were performed to determine the spin and recovery characteristics of the model for the normal-control configuration for spinning (elevator full up, ailerons neutral, and rudder full with the spin) and for various other aileron-elevator combinations including neutral and maximum settings of the surfaces for various model loadings and configurations. Recovery was generally attempted by rapid reversal of the rudder from full with to full against the spin. Recovery was also attempted by moving the ailerons to an intermediate or full deflection with the spin. For some tests, rudder reversal was accompanied by elevator reversal. Tests were also performed to evaluate the possible adverse effects of small deviations from the normal-control configuration for spinning. For these tests, the elevator was set at two-thirds of its full up deflection and the ailerons were set at one-third of full deflection in the direction conducive to slower recoveries (against the spin for this model for all loadings tested). This particular control configuration is referred to as the "criterion spin." Recovery from this spin was attempted by rapidly reversing the rudder from full with to only two-thirds against the spin or by reversing only the ailerons to with the spin.

The number of turns required for the spin rotation to cease was measured from the time the controls were moved until the rotation was terminated. Based on previous spin-tunnel experience, the spin rotation was considered to be adequately damped if the model stopped rotating within $2\frac{1}{4}$ turns after control movement from the criterion spin.

For recovery attempts in which the model struck the safety net while it was still in a spin, the recovery was recorded as greater than the number of turns from the time the controls were moved to the time the model struck the net. The condition existing when the spinning motion imparted to the model at launching was damped without movement of the controls is referred to as "No spin" on the charts.

Force tests.- The lift, drag, and pitching-moment data were obtained by mounting the models on a six-component electrical strain-gage balance in the Langley 20-foot free-spinning tunnel.

Glide tests.- In order to investigate the longitudinal trim tendencies of the $\frac{1}{20}$-scale model for rearward positions of the center of gravity, the model was launched from an improvised ramp at one side of the tunnel and permitted to glide freely across the tunnel, the tunnel airspeed being held constant. The attitude of the model during its flight across the tunnel was determined from studies of motion pictures of the model. Inasmuch as the transverse and vertical angles of the camera axis and the horizontal and vertical distances traversed by the model in a given time interval had to be estimated, the angle-of-attack data presented for these tests are of qualitative nature only.

PRECISION

The results presented herein are believed to be the true values given by the model within the following limits:

	Spin tests	Force tests
α, degree	± 1	± 0.5
ϕ, degree	± 1	----
V, percent	± 5	± 3
Ω, percent	± 2	----
Turns for recovery	$\pm\frac{1}{4}$	----

The preceding limits may have been exceeded for some of the spins which were difficult to control in the tunnel because of the wandering or oscillatory nature of the spin.

Comparison between model and full-scale spin results (references 1 and 2) indicates that spin-tunnel results are not always in complete agreement with airplane spin results. In general, the models spun at a somewhat higher rate of descent and at from 5° to 10° more outward sideslip than did the corresponding full-scale airplanes. The comparison made in reference 2 for 20 airplanes showed that 80 percent of the models predicted satisfactorily the corresponding full-scale recovery characteristics and that 10 percent overestimated and 10 percent underestimated the corresponding full-scale recovery characteristics.

The limits of accuracy of the electrical-strain-gage measurements are believed to be as follows:

	$\frac{1}{12}$-scale model	$\frac{1}{20}$-scale model
C_L	±0.023	±0.041
C_D	±0.015	±0.027
C_m	±0.007	±0.021

As has been explained previously, the glide data presented herein are considered only qualitative because the attitude of the model could not be measured accurately.

The accuracies of measuring the weight and mass distribution of the model are believed to be within the following limits:

Weight, percent	±1
Center-of-gravity location, percent $\bar{c}$	±1
Moments of inertia, percent	±5

Control settings are made with an accuracy of ±1°.

TEST CONDITIONS

Tests were performed for the model conditions listed in table II. For all tests, the landing gear was retracted and the cockpit was closed. The mass-distribution parameters for the loadings tested on the model are tabulated in table III and plotted in figure 5.

The maximum control deflections used in the tests were:

Rudder, degrees:	
Right	30
Left	30
Elevons, degrees:	
As elevators,	
Up	20
Down	20
As ailerons,	
Up	15
Down	15

The same maximum control deflections were used for all the various vertical-tail configurations tested. Figure 6 shows the angular deflections of the elevons plotted against stick position.

The force tests were made at a q of 7.9 pounds per square foot with a corresponding Reynolds number of 0.45×10^6 for the $\frac{1}{20}$-scale model. For the force tests on the $\frac{1}{12}$-scale model, q varied from 4.2 to 5.3 pounds per square foot, the corresponding variation in Reynolds number being from 0.53×10^6 to 0.59×10^6. The tunnel speed (and the Reynolds number) had to be reduced at the higher angles of attack for the $\frac{1}{12}$-scale-model tests to prevent the model from vibrating. The turbulence factor of the spin tunnel is 1.8. No tunnel-wall or blocking corrections have been applied to the force data because of the small size of the models relative to the diameter of the tunnel.

DISCUSSION

Single-Vertical-Tail Configuration

Spin tests.- The results of the spin tests for the model with the single-vertical-tail configuration, which was loaded to represent an assumed normal loading for the corresponding full-scale airplane, are shown in chart 1. For this loading the center of gravity was positioned at 24 percent of the mean aerodynamic chord, and the inertia yawing-moment parameter $\frac{I_X - I_Y}{mb^2}$ and the relative density were equivalent to -754×10^{-4} and 21.93, respectively (model loading 7 in table III and fig. 5). As is shown in chart 1, the model would not spin for any control configuration. For the normal-control configuration for spinning (elevator up, ailerons neutral, and rudder full with the spin), the launching rotation was expended rapidly but the model appeared to remain in a flat stalled glide. When the elevator and ailerons were neutral, the model dived vertically, and when the elevator was down the model pitched inverted. With the ailerons set full against the spin, the spinning rotation imparted on launching was damped very rapidly and a rolling oscillation started which increased in magnitude until the model rolled continuously about the longitudinal body axis. The angle between the longitudinal body axis and the air stream usually appeared to be well above the stall angle when the elevator was up, neutral, or down. With the ailerons set at one-third of their full deflection against the spin, the rolling motion was again evident, commencing simultaneously with the cessation of the forced-spin rotation. Strip-film motion-picture records

showing the cessation of the hand-forced-spin rotation and the ensuing rolling motion are shown in figure 7. When the ailerons were set with the spin, the results were similar to those obtained with the ailerons at neutral.

The effects of varying the relative density and the mass distribution, the center of gravity being held constant at the normal position, are shown in chart 2. As can be seen from this chart, there is a region in which the model did not spin which extends from a value of the inertia yawing-moment parameter equal to somewhat less negatively than -450×10^{-4} to a value somewhat greater negatively than -750×10^{-4}; however, the model still appeared to remain at attitudes above the stall for all elevator-up settings and all aileron-against settings after the launching rotation ceased. When the value of the inertia yawing-moment parameter was increased to approximately -70×10^{-4} or decreased to approximately -1000×10^{-4}, spins were obtained usually when the ailerons were set against the spin; decreasing the value of the inertia yawing-moment parameter to approximately -1500×10^{-4} led to spins when the ailerons were neutral as well as when they were against the spin. The spins obtained were generally flat and the reversal of the rudder was generally not effective in terminating the spin rotation if the ailerons were even partially against the spin. Spins obtained with ailerons neutral could be terminated by rudder reversal. The data presented in chart 2 indicate that there was little difference in the results obtained for the three values of relative density tested.

In order to terminate the rotation of the spins obtained with the ailerons either partially or fully against the spin, recoveries were attempted by moving the ailerons from against to with the spin, rudder and elevator remaining fixed at their initial settings, or by simultaneously reversing both the rudder and elevator, the ailerons remaining fixed. The results of these tests, presented in table IV for a few representative loadings, indicate that reversal of both rudder and elevator was not effective in terminating the spin rotation, whereas movement of the ailerons to full with the spin was effective. The results indicated that, although movement of the ailerons partially with the spin would be beneficial, in order to insure termination of the spin rotation for all loadings the ailerons should be moved full with the spin. It appears that within the range of loadings tested, the ailerons instead of the rudder and elevator will be the most effective controls for terminating the spin rotation of airplanes corresponding to the model tested.

Comparison of the results of tests presented on charts 3 and 4, with those presented on charts 1 and 2 shows the effects of moving the center of gravity rearward from normal to 30 and 35 percent of the mean aerodynamic chord. These tests were conducted at two mass distributions: a mass distribution for which no spins had been obtained at the normal

center-of-gravity location and a mass distribution for which the model exhibited strong spinning tendencies at the normal center-of-gravity location. When the center of gravity was moved rearward the model spun when the ailerons were placed against the spin, but the model still resisted spinning when the ailerons were placed with the spin. As had usually been the case when spins were obtained at the normal center-of-gravity location when the ailerons were against the spin, rudder reversal was again ineffective in terminating the spin rotation; and, although not specifically tested for all conditions, it appeared that movement of the ailerons to full with the spin would have been effective in damping the spin rotation. This conclusion was based on the similarity of the spin characteristics for these tests and for those conducted at the normal center-of-gravity location. (See table IV.) For those control settings for which the model did not spin, or for the spins which were terminated by movement of the controls, the model generally appeared to remain above the stall after the termination of the rotation. As is indicated in charts 3 and 4, when the center of gravity was at 30 percent of the mean aerodynamic chord, the elevator had to be set to 10° down before the model was observed to dive out of its apparent flat glide, and when the center of gravity was at 35 percent of the mean aerodynamic chord the elevator had to be set at 60° down in order to make the model pitch to an unstalled attitude.

Static-force tests and glide tests.- The behavior of the model used in this investigation during its recovery from a spin was different from that of a conventional model. Generally, the attitude of a conventional model steepens as the rotation slows down after movement of the controls for recovery so that the model is almost vertical by the time the rotation has been terminated. The attitude of the model used in this investigation did not begin to steepen until after the rotation had been terminated and the model had begun to glide. The flight of the model could be observed for a time duration corresponding to about 2.5 seconds on a full-scale airplane from the time the rotation was terminated until the model struck the safety net, so that a very slow change in attitude from a flat stalled to an unstalled angle of attack would not be observable in the tunnel, and the model would thus appear to remain at its initial highly stalled attitude. Accordingly, force tests were conducted to determine the trim attitudes that might be experienced by a delta-wing airplane having design characteristics similar to the model tested for the range of center-of-gravity positions investigated in the spin tests. As previously indicated, force tests were conducted on the $\frac{1}{20}$-scale model used for the spin tests. Because the pitching-moment data derived from the $\frac{1}{20}$-scale-model tests were of about the same order of magnitude as the precision of the measurements, force tests were also made on a larger model which was available and which was considered to

be a $\frac{1}{12}$-scale representation of a corresponding full-scale fighter-type airplane. A comparison plot of the aerodynamic characteristics in pitch of the $\frac{1}{12}$-scale and $\frac{1}{20}$-scale models and of a full-scale airplane previously tested by the NACA, which airplane is generally similar to the models tested, is shown in figure 8. As can be seen from this figure, the pitching-moment curves of the full-scale airplane and the two models show general agreement, although the trim angle indicated by the $\frac{1}{20}$-scale model differed somewhat from that indicated by the full-scale and $\frac{1}{12}$-scale-model data. The greater portion of the force data presented in this paper is for the $\frac{1}{12}$-scale model inasmuch as the pitching-moment characteristics of this model were somewhat more like those of the full-size airplane.

Figures 9 and 10 indicate that the $\frac{1}{12}$-scale model will not trim above the stall for neutral or down positions of the elevators even when the center of gravity is as far rearward as 35 percent of the mean aerodynamic chord. When the center of gravity is at 35 percent of the mean aerodynamic chord, the model is approximately neutrally stable. Inasmuch as the slopes of the pitching-moment curves are rather flat, particularly when the center of gravity is rearward of normal, a corresponding full-scale airplane might be expected to be slow in changing attitude from a high stalled angle of attack to an unstalled condition for rearward positions of the center of gravity. This expectation is borne out by the results of the spin tests of the $\frac{1}{20}$-scale model.

Because the $\frac{1}{20}$-scale model traversed only a relatively short distance during the ensuing glide after the termination of the spin rotation (usually about half the diameter of the tunnel), a few glide tests were made so that a greater portion of the glide could be observed by permitting the model to glide all the way across the tunnel. The results of these tests are presented in figure 11 and indicate that the rate of change of angle of attack from an initial stalled condition to an unstalled attitude was rather slow when the elevator was neutral and the center of gravity was at 30 percent of the mean aerodynamic chord. When the elevator was up, with the center of gravity at 30 percent $\bar{c}$, and when the elevator was neutral or up, with the center of gravity at 35 percent $\bar{c}$, the glide data indicate that the model tended to trim above the stall. These results are generally consistent with those predicted by the $\frac{1}{12}$-scale-model force data.

It appears from the test results that although a delta-wing-airplane configuration similar to the models used for this investigation will probably not exhibit any trim conditions above the stall unless the elevator is up or the center of gravity is so far rearward that the airplane is almost neutrally stable, the rate of change in angle of attack from a high stalled angle of attack to an unstalled attitude may be slow unless the center of gravity is maintained forward of approximately 25 percent of the mean aerodynamic chord. In addition, there is the possibility that the stick force required to move the stick forward to or beyond neutral when the airplane is at a high stalled attitude may exceed the pilot's capabilities, and it may be desirable to install a boost apparatus in the control system to assist the pilot in moving the controls.

Multiple-Vertical-Tail Configuration

In order to determine the effects of other vertical-tail configurations on the spin and recovery characteristics of designs of this type, the model was tested with several dual-vertical-tail arrangements. For these tests small dual vertical tails were added at the wing tips of the model, the center tail being retained, and, in addition, the model was tested with the single vertical tail removed and two larger sets of dual vertical tails alternately added to the wing tips. These tail arrangements are shown in figure 2. The small dual vertical tails were not tested alone because they were considered inadequate to provide the desired amount of directional stability, whereas the other two larger sets of dual tails were deemed capable of providing a directionally stable aircraft. The results of the tests are presented on charts 5 and 6. The tests were conducted at two loading conditions, one with the center of gravity at 30 percent of the mean aerodynamic chord (loading 15 in table III and fig. 5) and the other with the center of gravity at 35 percent of the mean aerodynamic chord (loading 16 in table III and fig. 5), with moments of inertia corresponding to those tested at the normal loading. The results with the single vertical tail installed showed that the effects of moving the center of gravity rearward from normal (moments of inertia maintained at their normal values) were similar to the effects obtained by increasing or decreasing the value of the inertia yawing-moment parameter from normal. It is expected that somewhat similar effects may exist with the multitail arrangements installed on the model. Thus it appears that the results of tests at the two center-of-gravity positions investigated may give a general indication of the results that might be expected at other mass distributions.

As is shown in chart 5, when the center of gravity was at 30 percent of the mean aerodynamic chord, all the multitail arrangements contributed sufficient damping to prevent the attainment of a condition of spin equilibrium for all control settings except the normal spin-control

configuration. The results indicated, however, that reversal of the rudders alone would terminate the spin rotation for this spin. When the center of gravity was moved rearward to 35 percent of the mean aerodynamic chord, however, the small-dual- and single-vertical-tail combination did not appear to terminate satisfactorily the spin rotation for the criterion spin-control configuration by reversal of the rudders, whereas the two large dual-tail arrangements were still generally effective in terminating the rotation. The results indicate that the large-dual-vertical-tail arrangements were more effective in damping the spin rotation than the combination of small dual tails and single center tail, or the single vertical tail alone, and, further, that with either of the large-dual-vertical-tail arrangements installed (22 and 27 percent of the wing area, respectively) the spin rotation could be terminated by reversal of the rudders. Addition of the dual vertical tails, however, did not eliminate the undesirable characteristics in pitch for rearward positions of the center of gravity.

CONCLUSIONS

Based on dynamic and static tests of 60° delta-wing models, the following conclusions for a similar full-scale airplane are made:

1. Spins obtained will generally be flat and reversal of the rudder will generally be ineffective in terminating the spin rotation. Use of twin vertical tails of sufficient size will be effective in stopping the spin rotation but the airplane may tend to remain in a flat stalled attitude and it will be necessary to move the stick forward of neutral in order to pitch rapidly to an unstalled attitude.

2. In general, moving the ailerons to full with the spin will be the most effective control movement for terminating the spin rotation.

3. Spins may not be obtained for a range of values of the inertia yawing-moment parameter extending from approximately -450×10^{-4} to -750×10^{-4}.

4. Rearward positions of the center of gravity will increase the likelihood of obtaining spins and will require larger elevator-down settings to pitch the airplane rapidly to an unstalled attitude. For

satisfactory longitudinal trim characteristics, it appears that the center of gravity should be maintained forward of the 25-percent station of the mean aerodynamic chord.

5. There will be little effect on spin and recovery characteristics of changes in airplane relative density.

Langley Aeronautical Laboratory
National Advisory Committee for Aeronautics
Langley Air Force Base, Va.

REFERENCES

1. Zimmerman, C. H.: Preliminary Tests in the N.A.C.A. Free-Spinning Wind Tunnel. NACA Rep. 557, 1936.

2. Seidman, Oscar, and Neihouse, A. I.: Comparison of Free-Spinning Wind-Tunnel Results with Corresponding Full-Scale Spin Results. NACA MR, Dec. 7, 1938.

TABLE I.- DIMENSIONAL CHARACTERISTICS OF THE MODEL

[Model values are presented in terms of full-scale values]

	Single-vertical-tail configuration	Small-dual-vertical-tail and single-vertical-tail configurations	Medium-dual-vertical-tail configuration	Large-dual-vertical-tail configuration
Length, over all, ft	41.37	41.37	41.37	41.37
Wing:				
Span, ft	29.42	22.83	22.83	22.83
Area, sq ft	375.0	366.4	366.4	366.4
Section, parallel to airplane center line	Modified NACA $65_{(06)}$-006.5	Modified NACA $65_{(06)}$-006.5	Modified NACA $65_{(06)}$-006.5	Modified NACA $65_{(06)}$-006.5
Mean aerodynamic chord, ft	16.99	16.99	16.99	16.99
Leading edge $\bar{c}$ behind apex angle wing, in.	101.98	101.98	101.98	101.98
Sweepback of leading edge of wing, deg	60	60	60	60
Tip chord, in.	0	68.8	68.8	68.8
Root chord, in.	305.8	305.8	305.8	305.8
Wing dihedral, deg	0	0	0	0
Aspect ratio	2.32	1.42	1.42	1.42
Distance from 24 percent $\bar{c}$ to elevon hinge, ft	10.53	10.53	10.53	10.53
Distance from 24 percent $\bar{c}$ to rudder hinge, ft	11.86	[a]13.46	15.66	18.33
Taper ratio	0	0.224	0.224	0.224
Elevon:				
Chord behind hinge line (constant), in.	34.4	34.4	34.4	34.4
Area of each elevon behind hinge line, sq ft	33.2	25.7	25.7	25.7
Vertical tail:				
Total area, sq ft	67	117	81.2	100.35
Rudder area behind hinge line, sq ft	13.4	[a]12.4	21.4	21.8
Chord behind hinge line (constant), in.	19.2	21.0	20.0	20.0
Aspect ratio	1.15	1.0	1.58	1.73

[a]Dimensions given for dual-vertical tails.

TABLE II.- TABULATION OF TESTS MADE ON MODELS

(a) DYNAMIC TESTS

Loading	$\frac{I_X - I_Y}{mb^2}$	μ	$x/\bar{c}$	Model configuration	Data presented in -
Spin tests on $\frac{1}{20}$-scale model - recovery attempted by full rudder reversal					
7	-754×10^{-4}	21.92	0.240	Single vertical tail	Charts 1 and 2
1	-452	15.10	.240	Single vertical tail	Chart 2
2	-772	15.00	.248	Single vertical tail	Chart 2
3	-999	15.00	.253	Single vertical tail	Chart 2
4	-1524	15.10	.239	Single vertical tail	Chart 2
5	-76	22.20	.249	Single vertical tail	Chart 2
6	-491	22.20	.248	Single vertical tail	Chart 2
8	-1008	22.80	.255	Single vertical tail	Chart 2
9	-1565	22.60	.251	Single vertical tail	Chart 2
10	-70	30.20	.235	Single vertical tail	Chart 2
11	-480	30.30	.240	Single vertical tail	Chart 2
12	-761	30.30	.241	Single vertical tail	Chart 2
13	-1021	30.30	.236	Single vertical tail	Chart 2
14	-1431	30.20	.240	Single vertical tail	Chart 2
15	-749	22.90	.300	Single vertical tail	Chart 3
16	-697	22.90	.350	Single vertical tail	Chart 4
17	-1442	15.00	.350	Single vertical tail	Chart 4
15	-749	22.90	.300	Small dual vertical tails plus single vertical tail	Chart 5
16	-697	22.90	.350	Small dual vertical tails plus single vertical tail	Chart 6
15	-749	22.90	.300	Medium dual vertical tails	Chart 5
15	-749	22.90	.300	Large dual vertical tails	Chart 5
16	-697	22.90	.350	Medium dual vertical tails	Chart 6
16	-697	22.90	.350	Large dual vertical tails	Chart 6
Glide tests on $\frac{1}{20}$-scale model					
15	-749×10^{-4}	22.90	0.300	Single vertical tail	Figure 11
16	-697	22.90	.350	Single vertical tail	Figure 11

Loading	$\frac{I_X - I_Y}{mb^2}$	μ	$x/\bar{c}$	Model configuration	Controls moved for recovery	Data presented in -
Spin tests on $\frac{1}{20}$-scale model - recovery attempted by control movement indicated						
14	-143×10^{-4}	30.20	0.240	Single vertical tail	Rudder and elevator	Table IV
4	-1524	15.10	.239		Ailerons	
10	-70	30.20	.235		Ailerons	
13	-1021	30.30	.235		Ailerons	
14	-1431	30.20	.240		Ailerons	
15	-749	22.90	.300		Ailerons	

(b) STATIC TESTS

Vertical-tail configuration	$x/\bar{c}$	Model scale	Elevator setting, δ_e (deg)	Aileron setting, δ_a (deg)	Rudder setting, δ_r (deg)	Data presented	Data presented in -
Single vertical tail	0.240	1/20	0	0	0	C_L, C_D, C_m	Figure 8
		1/12	0	0	0		Figures 8 and 9
		1/12	20	0	0		Figure 9
		1/12	-20	0	0		Figure 9
	.240, .300, and .350	1/12	-20	0	0	C_m	Figure 10
		1/12	0	0	0		Figure 10
		1/12	20	0	0		Figure 10

NACA

TABLE III.- MASS CHARACTERISTICS AND INERTIA PARAMETERS FOR VARIOUS LOADINGS TESTED ON THE $\frac{1}{20}$-SCALE MODEL

[Model values are presented in terms of full-scale values; moments of inertia are given about center of gravity; model is in clean condition]

Loading	Weight (lb)	Relative airplane density μ		Center-of-gravity location		Moments of inertia (slug-feet^2)			Inertia parameters		
		Sea level	Altitude of 15,000 feet	$x/\bar{c}$	$z/\bar{c}$	I_X	I_Y	I_Z	$\frac{I_X - I_Y}{mb^2}$	$\frac{I_Y - I_Z}{mb^2}$	$\frac{I_Z - I_X}{mb^2}$
1	8,019	9.49	15.10	0.240	0.040	6,283	16,029	20,502	-452×10^{-4}	-207×10^{-4}	659×10^{-4}
2	8,002	9.47	15.00	.248	.013	2,301	18,914	20,497	-772	-74	846
3	7,980	9.44	15.00	.253	.032	2,714	24,157	25,330	-999	-55	1054
4	8,047	9.53	15.10	.239	.043	2,815	35,821	36,737	-1524	-42	1566
5	11,820	13.98	22.20	.249	.037	15,900	18,301	32,834	-76	-457	533
6	11,842	14.00	22.20	.248	.051	8,825	24,467	31,470	-491	-220	711
7	11,648	13.80	21.93	.240	.014	3,989	27,619	29,557	-754	-67	821
8	12,164	14.40	22.80	.255	.066	4,924	37,909	40,618	-1008	-83	1091
9	12,040	14.20	22.60	.251	.050	5,190	55,900	57,756	-1565	-57	1622
10	16,082	19.00	30.20	.235	.056	21,894	24,924	43,914	-70	-439	509
11	16,132	19.10	30.30	.240	.049	12,636	33,466	43,917	-480	-241	721
12	16,126	19.10	30.30	.241	.047	5,896	38,902	42,201	-761	-76	837
13	16,115	19.05	30.30	.236	.043	5,696	49,941	53,125	-1021	-73	1094
14	16,059	19.00	30.20	.240	.048	3,048	64,935	65,305	-1431	-9	1440
15	12,175	14.40	22.90	.300	-.0012	4,013	28,539	30,350	-749	-55	804
16	12,175	14.40	22.90	.350	.009	4,002	26,826	28,620	-697	-55	752
17	7,972	9.44	15.00	.350	.042	2,880	33,800	34,900	-1442	-51	1493

TABLE IV.- EFFECT OF VARIOUS CONTROL MOVEMENTS ON THE SPIN-RECOVERY CHARACTERISTICS OF THE $\frac{1}{20}$-SCALE MODEL

Loading (See table III and fig. 5)	$\frac{I_X - I_Y}{mb^2}$	Center of gravity $x/\bar{c}$	μ	Initial aileron setting	Initial elevator setting	Initial rudder setting	Turns for recovery
Aileron-reversal tests (ailerons reversed to full with the spin unless otherwise noted)							
4	-1524×10^{-4}	0.239	15.10	1/3 against	2/3 up	full with	3/4
10	-70	.235	30.20	full against	neutral	full with	$1\frac{1}{2}$, $1\frac{3}{4}$
10	-70	.235	30.20	full against	full up	full with	2
10	-70	.235	30.20	1/3 against	2/3 up	full with	1/2, 1/2
13	-1021	.236	30.30	1/3 against	2/3 up	full with	1/2, 1/2
14	-1431	.240	30.20	full against	full up	full with	$2\frac{1}{4}$, $2\frac{1}{4}$
14	-1431	.240	30.20	full against	neutral	full with	$2\frac{1}{2}$, $2\frac{1}{4}$
14	-1431	.240	30.20	1/3 against	2/3 up	full with	$1\frac{3}{4}$, $1\frac{1}{4}$
14	-1431	.240	30.20	1/3 against	full up	full with	1/2
14	-1431	.240	30.20	neutral	neutral	full with	1/2, 1/4
14	-1431	.240	30.20	1/3 against	2/3 up	full with	[a]2, [a]3, [a]$3\frac{1}{2}$
15	-749	.300	22.90	1/3 against	2/3 up	full with	1/2
15	-749	.300	22.90	1/3 against	full up	full with	1
Simultaneous rudder- and elevator-reversal test (rudder and elevators reversed to full against the spin and to full down, respectively)							
14	-1431	.240	30.20	1/3 against	full up	full with	∞
14	-1431	.240	30.20	1/3 against	2/3 up	full with	∞

[a]Ailerons reversed to only 1/3 with the spin.

NACA

Chart 1.– SPIN CHARACTERISTICS OF MODEL FOR THE NORMAL LOADING; SINGLE VERTICAL TAIL INSTALLED AND CENTER OF GRAVITY AT 24 PERCENT $\bar{c}$

[Loading 7 in table III and figure 5 $\left(\frac{I_X - I_Y}{mb^2} = -754 \times 10^{-4};\ \mu = 21.93\right)$; model launched in an erect attitude with the rudder fixed full with the direction of rotation; rotation to pilot's right]

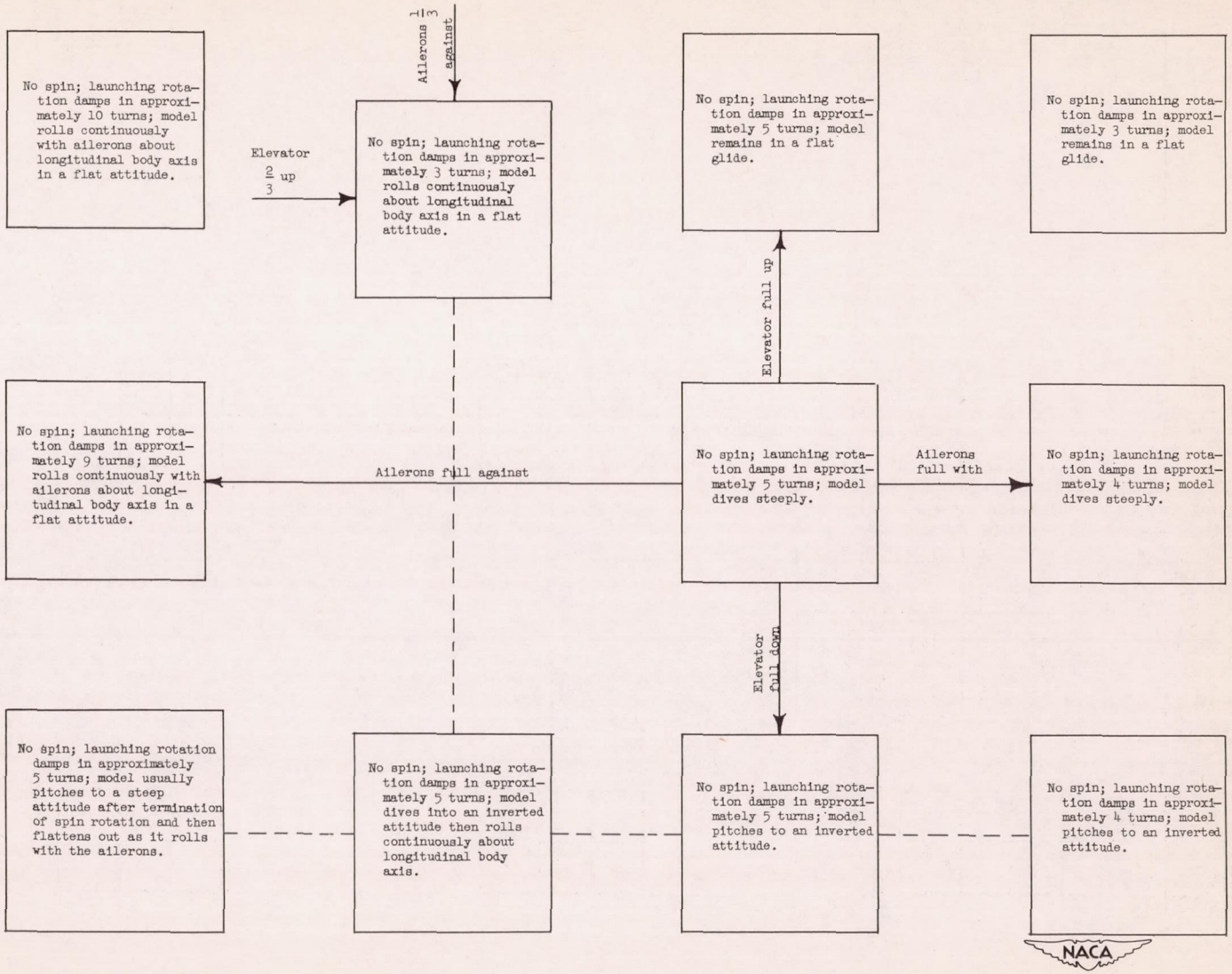
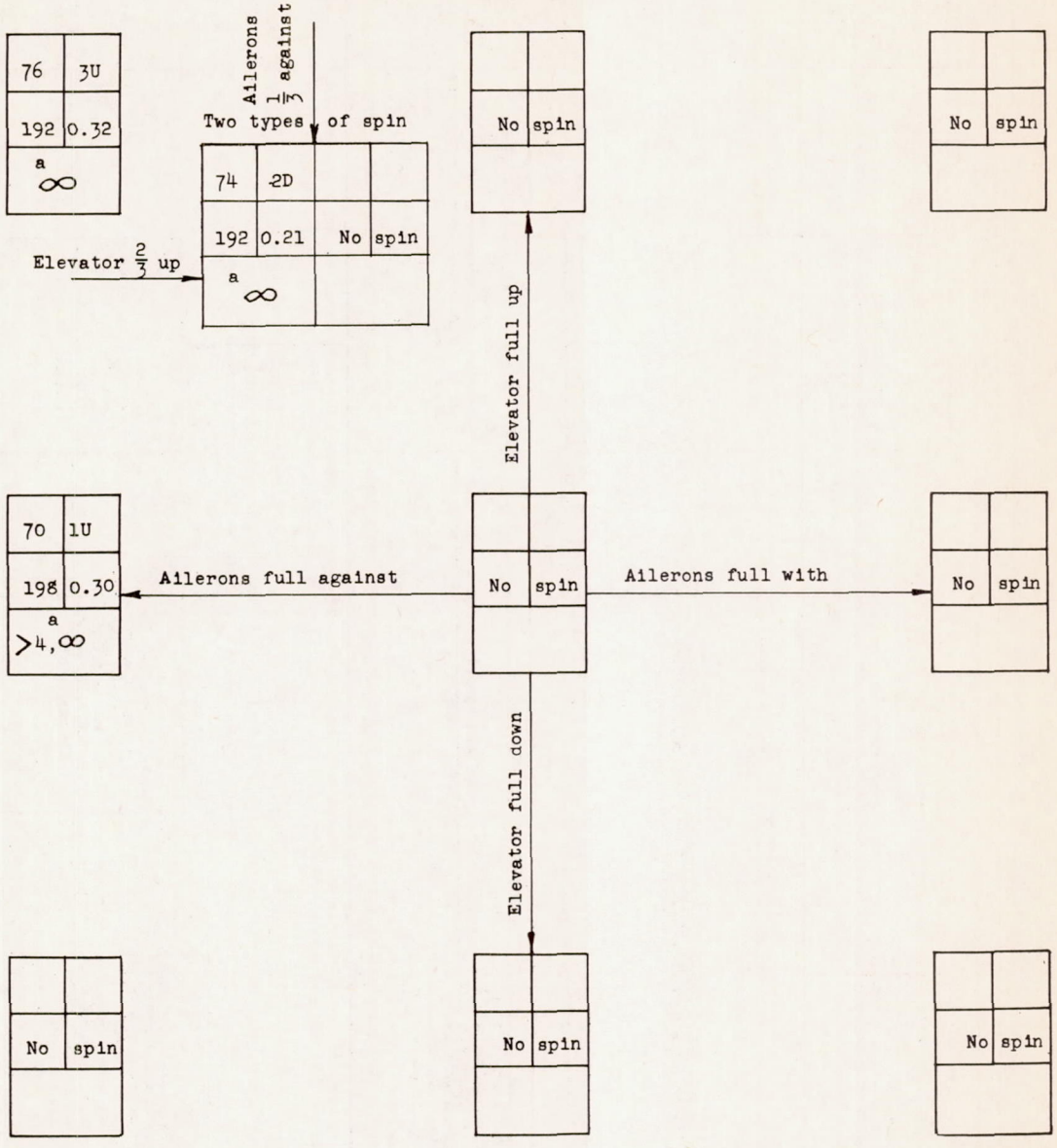


CHART 2(a).- SPIN CHARACTERISTICS OF MODEL FOR A LARGE RANGE OF INERTIA PARAMETERS AND RELATIVE DENSITIES; SINGLE VERTICAL TAIL INSTALLED AND CENTER OF GRAVITY AT 24 PERCENT $\bar{c}$

[Loading as indicated; model launched in an erect attitude with rudder fixed full with the direction of rotation; recoveries attempted by reversing the rudder from full with to full against the spin unless otherwise indicated; rotation to pilot's right. For control configurations for which "No spin" recorded, see chart 1 for description of model motion after launching rotation expended]

$\frac{I_X - I_Y}{mb^2} = -76 \times 10^{-4}$; $\mu = 22.20$

(Loading 5 in table III and fig. 5)



[a]Rudder reversed from full with to $\frac{2}{3}$ against the spin.

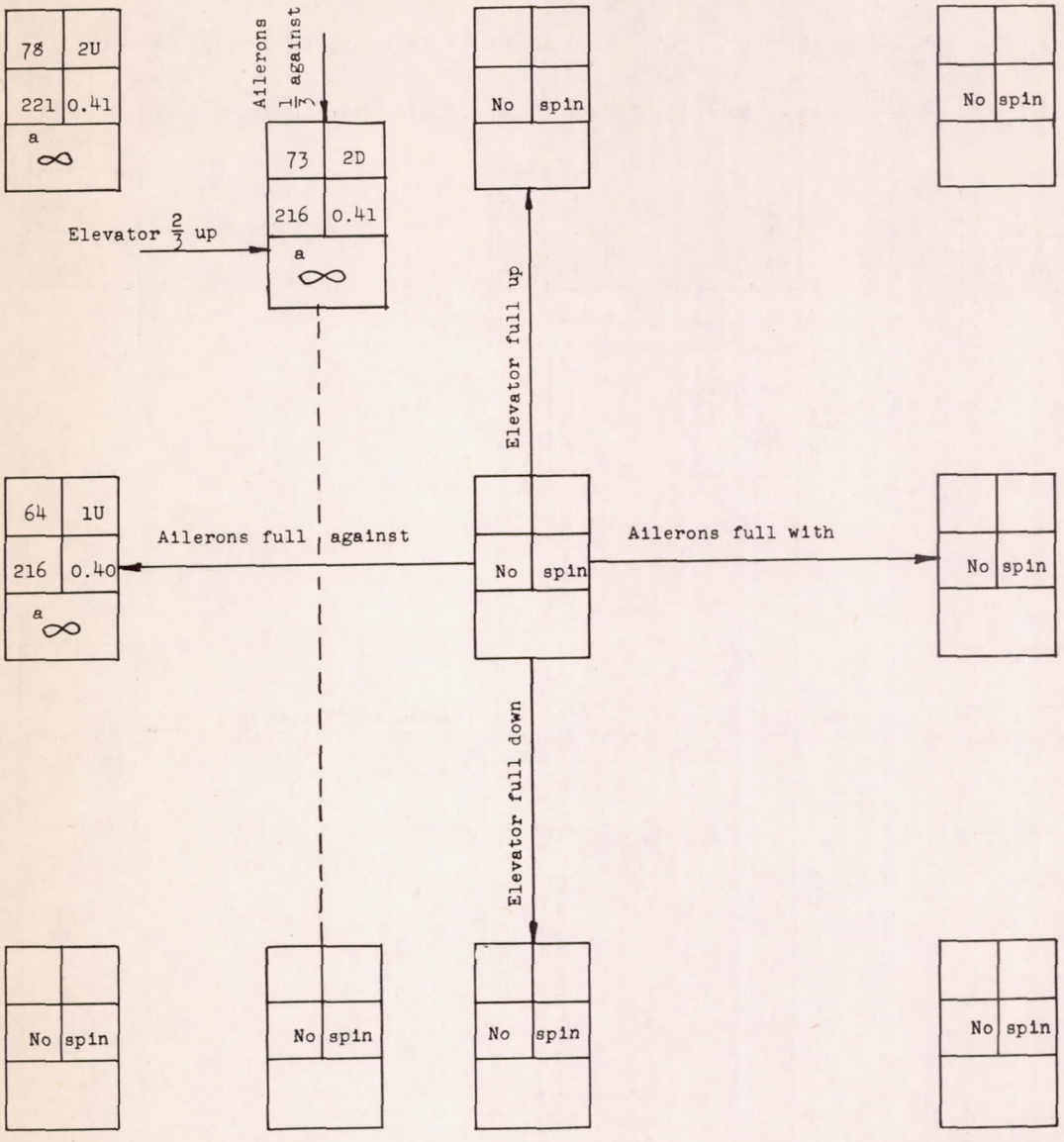
Model values converted to corresponding full-scale values.
U inner wing up
D inner wing down
∞ greater than 10 turns

NACA

CHART 2(a).- SPIN CHARACTERISTICS OF MODEL FOR A LARGE RANGE OF INERTIA PARAMETERS AND RELATIVE DENSITIES; SINGLE VERTICAL TAIL INSTALLED AND CENTER OF GRAVITY AT 24 PERCENT $\bar{c}$ - Concluded

$\frac{I_X - I_Y}{mb^2} = -70 \times 10^{-4}$; $\mu = 30.20$

(Loading 10 in table III and fig. 5)



[a] Rudder reversed from full with to $\frac{2}{3}$ against the spin.

Model values converted to corresponding full-scale values.
U inner wing up
D inner wing down
∞ greater than 10 turns

α (deg)	ϕ (deg)
V (fps)	Ω (rps)
Turns for recovery	

NACA

CHART 2(b).- SPIN CHARACTERISTICS OF MODEL FOR A LARGE RANGE OF INERTIA PARAMETERS AND RELATIVE DENSITIES; SINGLE VERTICAL TAIL INSTALLED AND CENTER OF GRAVITY AT 24 PERCENT $\bar{c}$

[Loading as indicated; model launched in an erect attitude with the rudder fixed full with the direction of rotation; rotation to pilot's right. For configurations for which "No spin" recorded, see chart 1 for description of model motion after launching rotation expended]

$\frac{I_X - I_Y}{mb^2} = -452 \times 10^{-4}$; $\mu = 15.10$ (loading 1 in table III and fig. 5),

$\frac{I_X - I_Y}{mb^2} = -491 \times 10^{-4}$; $\mu = 22.20$ (loading 6 in table III and fig. 5), and

$\frac{I_X - I_Y}{mb^2} = -480 \times 10^{-4}$; $\mu = 30.30$ (loading 11 in table III and fig. 5)

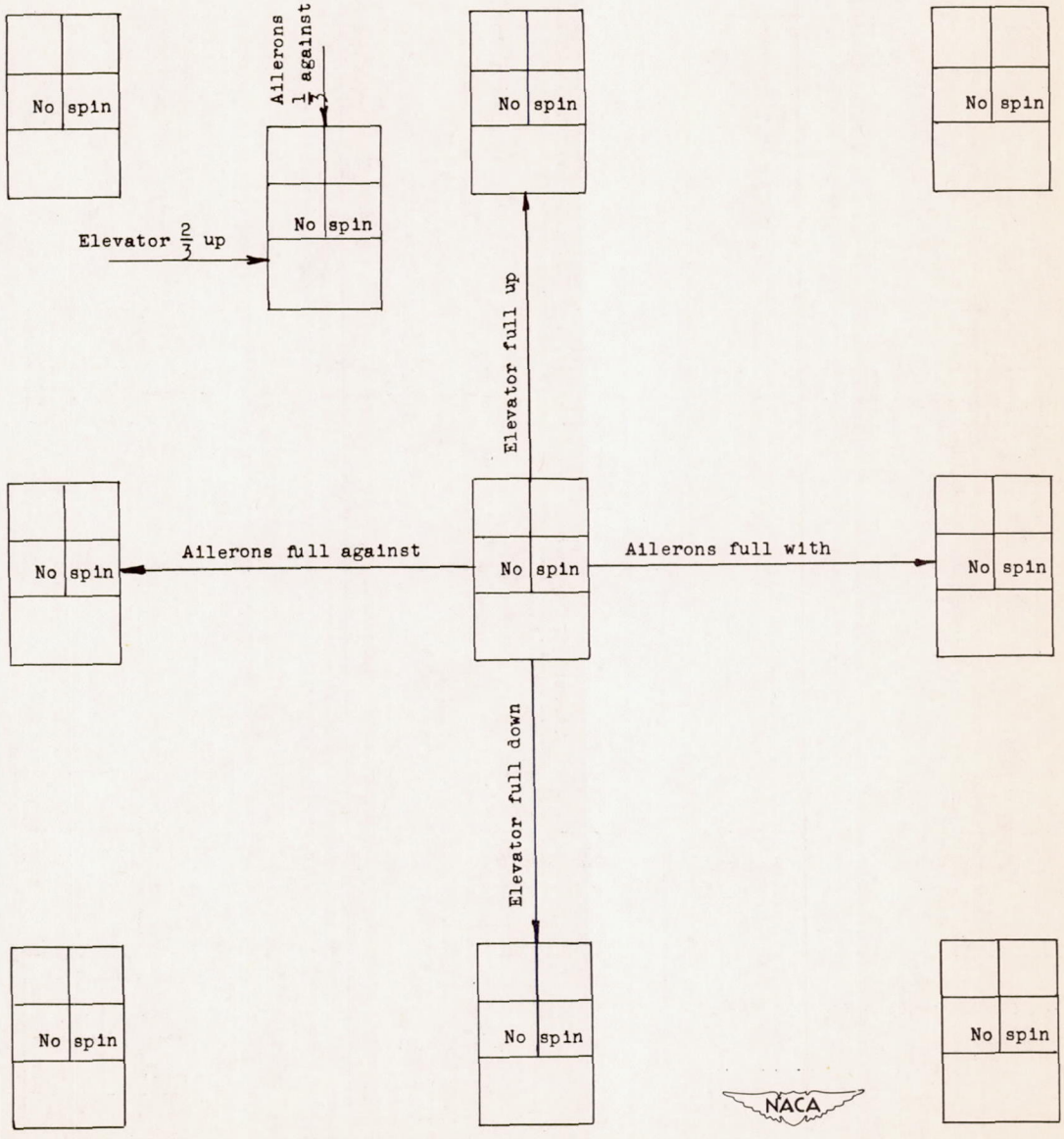


CHART 2(c).- SPIN CHARACTERISTICS OF MODEL FOR A LARGE RANGE OF INERTIA PARAMETERS AND RELATIVE DENSITIES; SINGLE VERTICAL TAIL INSTALLED AND CENTER OF GRAVITY AT 24 PERCENT $\bar{c}$

[Loading as indicated; model launched in an erect attitude with the rudder fixed with the direction of rotation; rotation to pilot's right. For control configuration for which "No spin" recorded, see chart 1 for description of model motion after launching rotation expended]

$\frac{I_X - I_Y}{mb^2} = -772 \times 10^{-4}$; $\mu = 15.00$ (loading 2 in table III and fig. 5),

$\frac{I_X - I_Y}{mb^2} = -754 \times 10^{-4}$; $\mu = 21.93$ (loading 7 in table III and fig. 5), and

$\frac{I_X - I_Y}{mb^2} = -761 \times 10^{-4}$; $\mu = 30.30$ (loading 12 in table III and fig. 5)

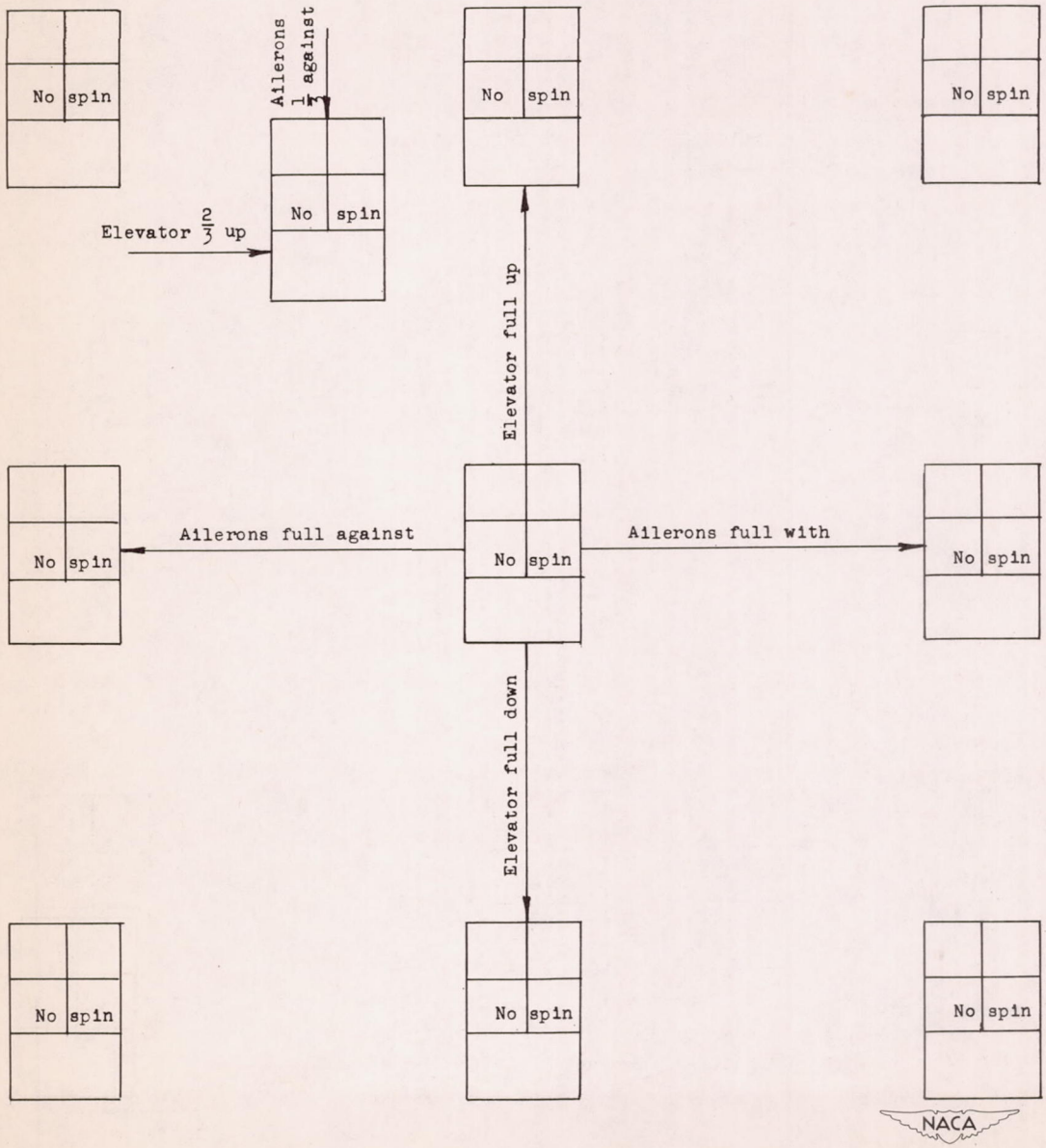
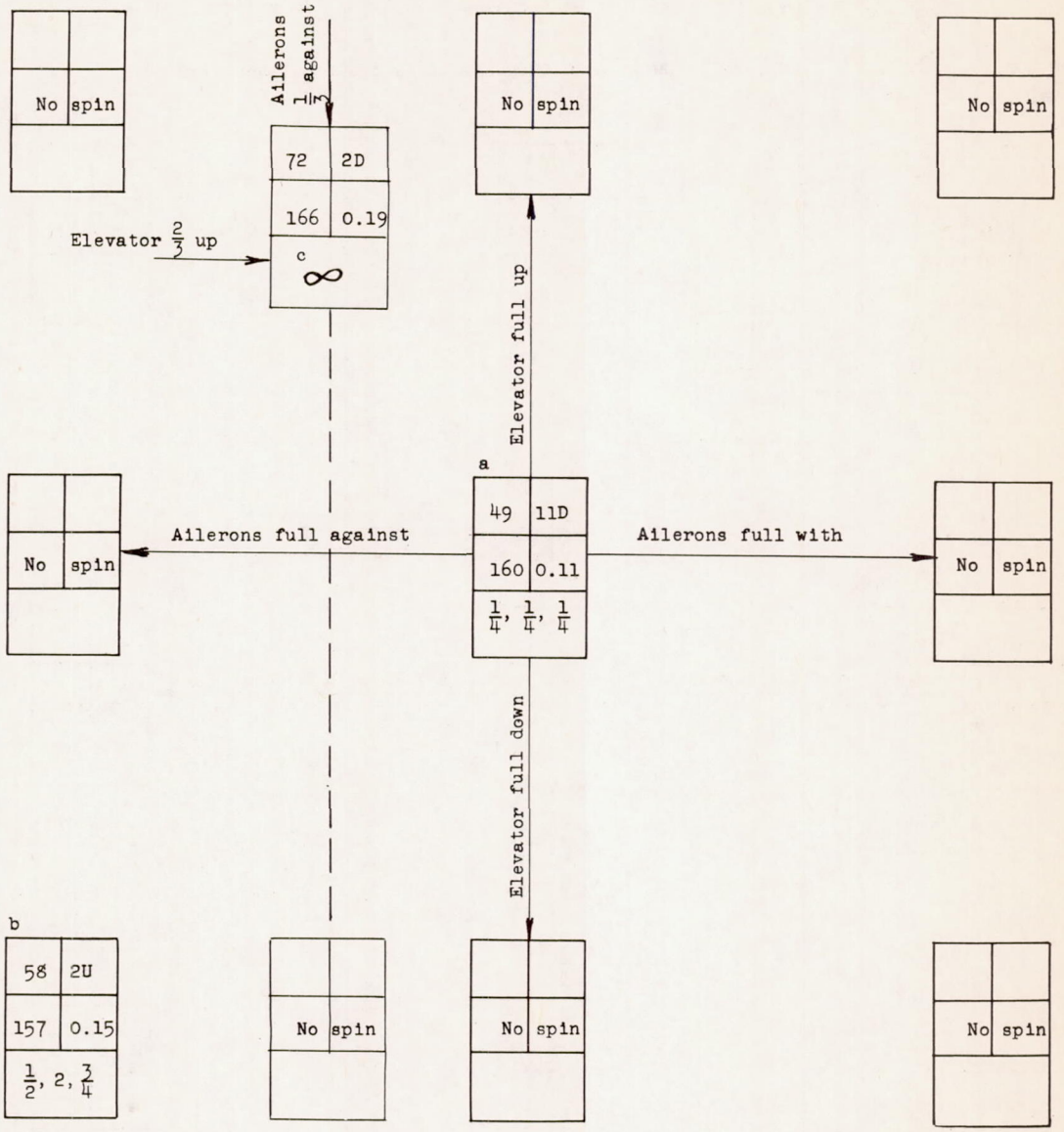


CHART 2(d).- SPIN CHARACTERISTICS OF MODEL FOR A LARGE RANGE OF INERTIA PARAMETERS AND RELATIVE DENSITIES; SINGLE VERTICAL TAIL INSTALLED AND CENTER OF GRAVITY AT 24 PERCENT $\bar{c}$

Loading as indicated; model launched in erect attitude with the rudder fixed full with the direction of rotation; recoveries attempted by reversing the rudder from full with to full against the spin unless otherwise noted; rotation to pilot's right. For control configurations for which "No spin" recorded, see chart 1 for description of model motion after launching rotation expended

$\frac{I_X - I_Y}{mb^2} = -999 \times 10^{-4}$; $\mu = 15.00$

(Loading 3 on table III and fig. 5)



[a]Wide radius spin.

[b]Model has a whipping motion as it spins.

[c]Rudder reversed from full with to 2/3 against the spin.

Model values converted to corresponding full-scale values.
U inner wing up
D inner wing down
∞ greater than 10 turns

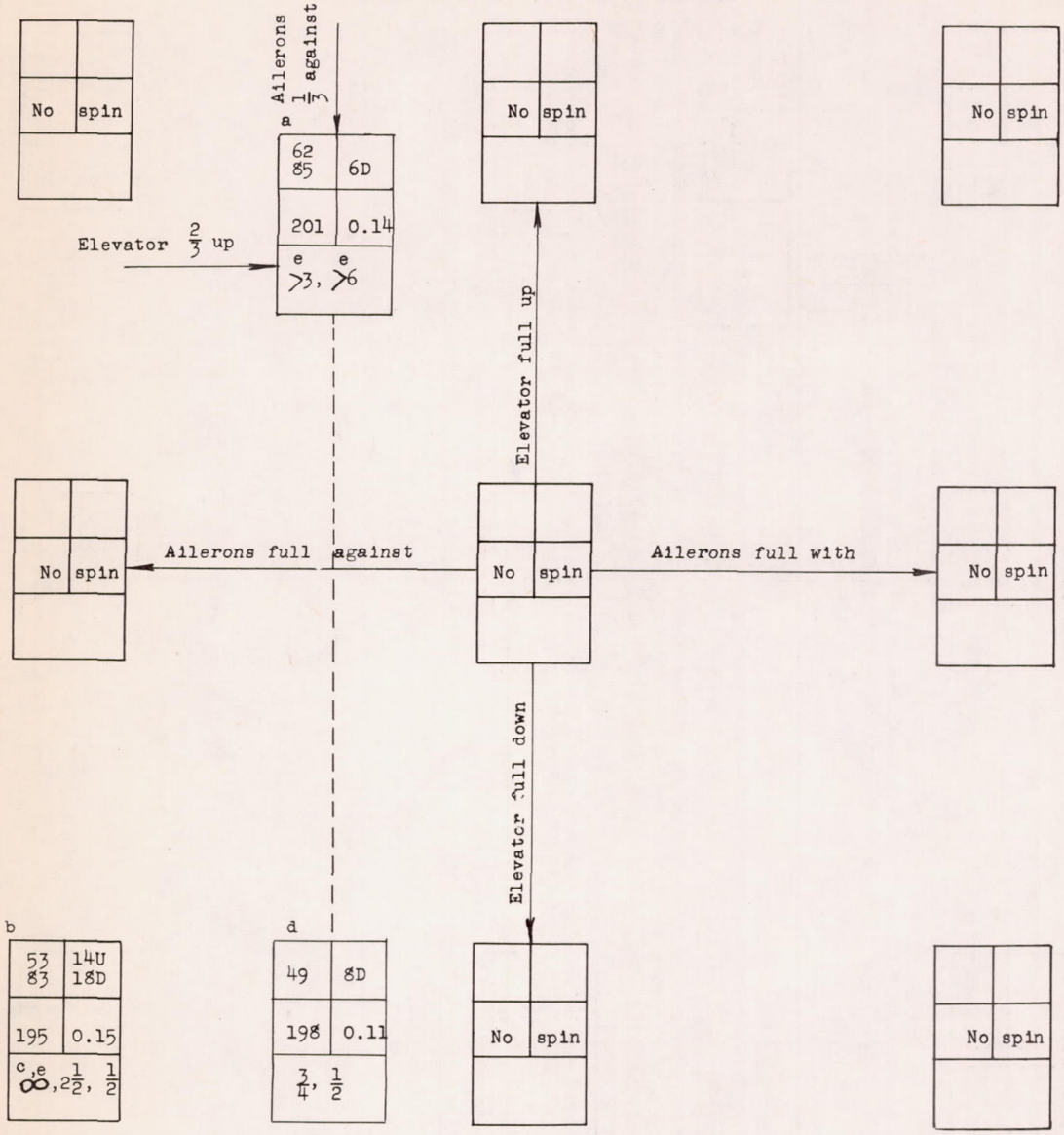
α (deg)	ϕ (deg)
V (fps)	Ω (rps)
Turns for recovery	

NACA

CHART 2(d).- SPIN CHARACTERISTICS OF MODEL FOR A LARGE RANGE OF INERTIA PARAMETERS AND RELATIVE DENSITIES; SINGLE VERTICAL TAIL INSTALLED AND CENTER OF GRAVITY AT 24 PERCENT $\bar{c}$ - Continued

$\frac{I_X - I_Y}{mb^2} = -1008 \times 10^{-4}$; $\mu = 22.80$

(Loading 8 on table III and fig. 5)



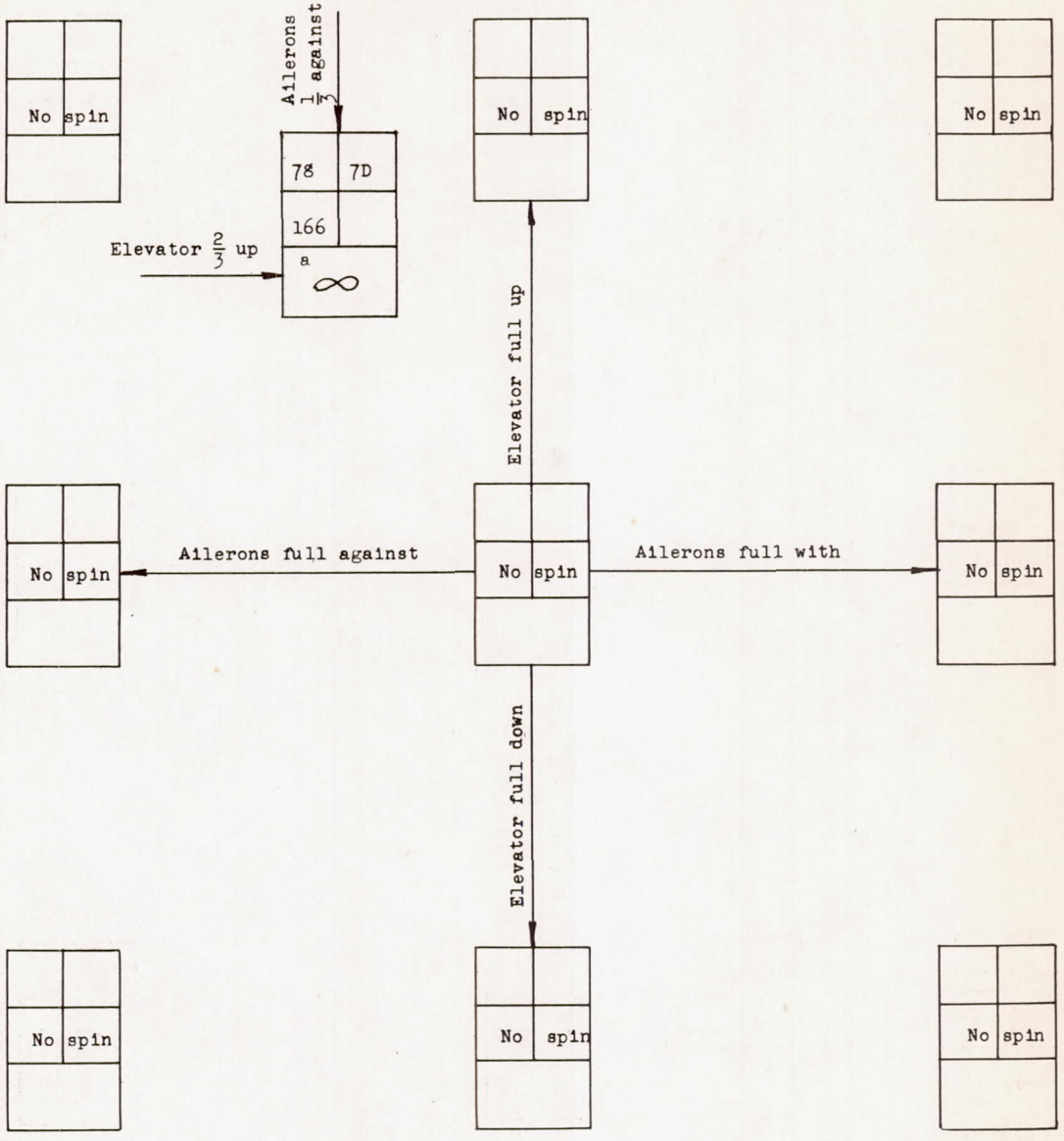
[a] Model oscillates in pitch.
[b] Model oscillates greatly in pitch and roll.
[c] Model in flat attitude when rudder was reversed.
[d] Wide radius spin.
[e] Rudder reversed from full with to $\frac{2}{3}$ against the spin.

Model values converted to corresponding full-scale values.
U inner wing up
D inner wing down

CHART 2(d).- SPIN CHARACTERISTICS OF MODEL FOR A LARGE RANGE OF INERTIA PARAMETERS AND RELATIVE DENSITIES; SINGLE VERTICAL TAIL INSTALLED AND CENTER OF GRAVITY AT 24 PERCENT $\bar{c}$ - Concluded

$\frac{I_X - I_Y}{mb^2} = -1021 \times 10^{-4}$; $\mu = 30.30$

(Loading 13 on table III and fig. 5)



[a] Rudder reversed from full with to ⅔ against the spin.

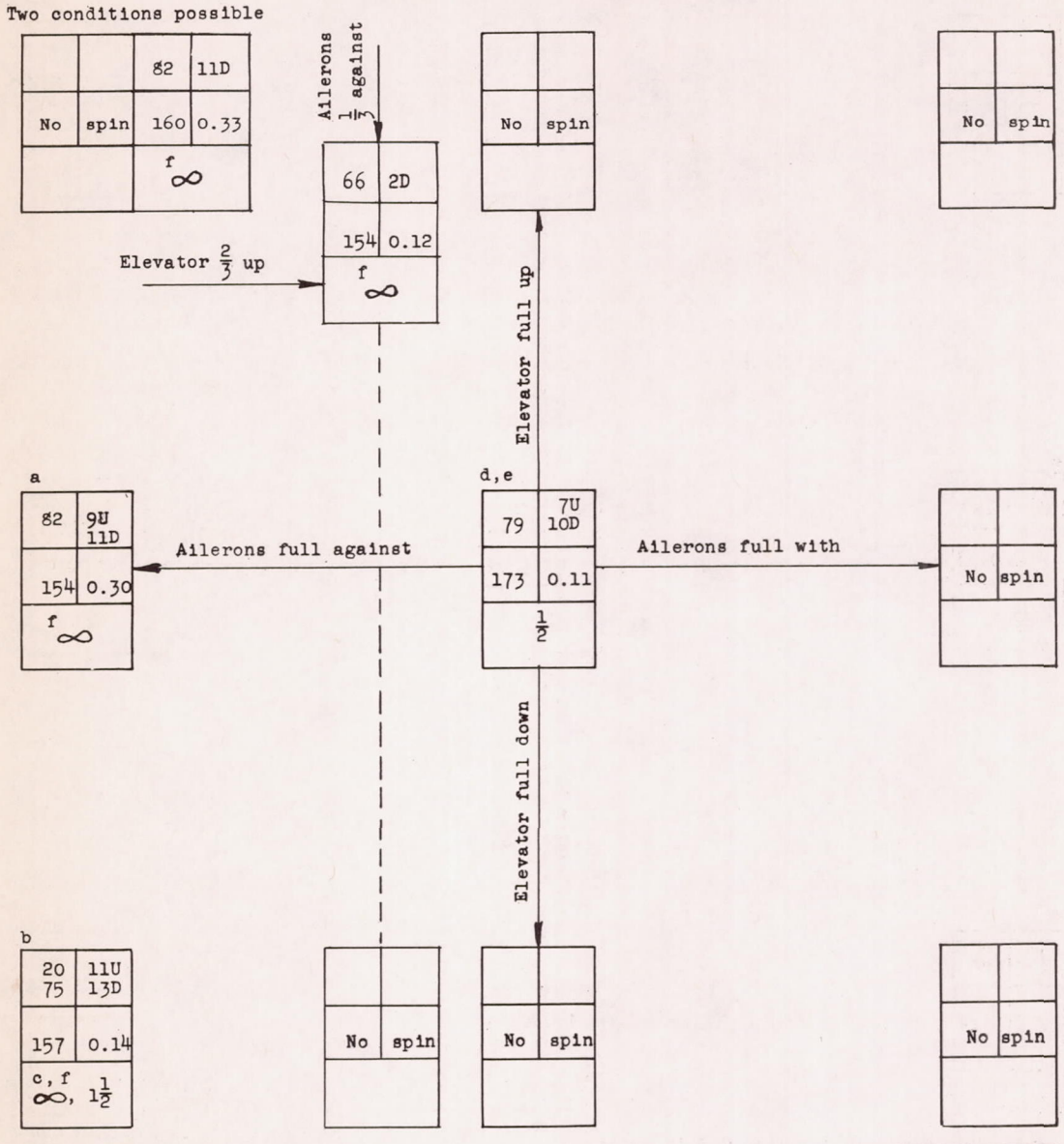
Model values converted to corresponding full-scale values.
U inner wing up
D inner wing down
∞ greater than 10 turns

CHART 2(e).- SPIN CHARACTERISTICS OF MODEL FOR A LARGE RANGE OF INERTIA PARAMETERS AND RELATIVE DENSITIES; SINGLE VERTICAL TAIL INSTALLED AND CENTER OF GRAVITY AT 24 PERCENT $\bar{c}$

[Loading as indicated; model launched in an erect attitude with the rudder fixed full with the direction of rotation; recoveries attempted by reversing the rudder from full with to full against the spin unless otherwise noted; rotation to pilot's right. For control configurations for which "No spin" recorded, see chart 1 for description of model motion after launching rotation expended]

$\frac{I_X - I_Y}{mb^2} = -1524 \times 10^{-4}$; $\mu = 15.10$

(Loading 4 in table III and fig. 5)



[a] Model has periodic oscillations in roll.
[b] Model oscillates greatly in pitch and roll.
[c] Rudder reversed while model in flat attitude.
[d] Wide radius spin.
[e] Wandering spin.
[f] Rudder reversed from full with to 2/3 against the spin.

Model values converted to corresponding full-scale values.
U inner wing up
D inner wing down
∞ greater than 10 turns

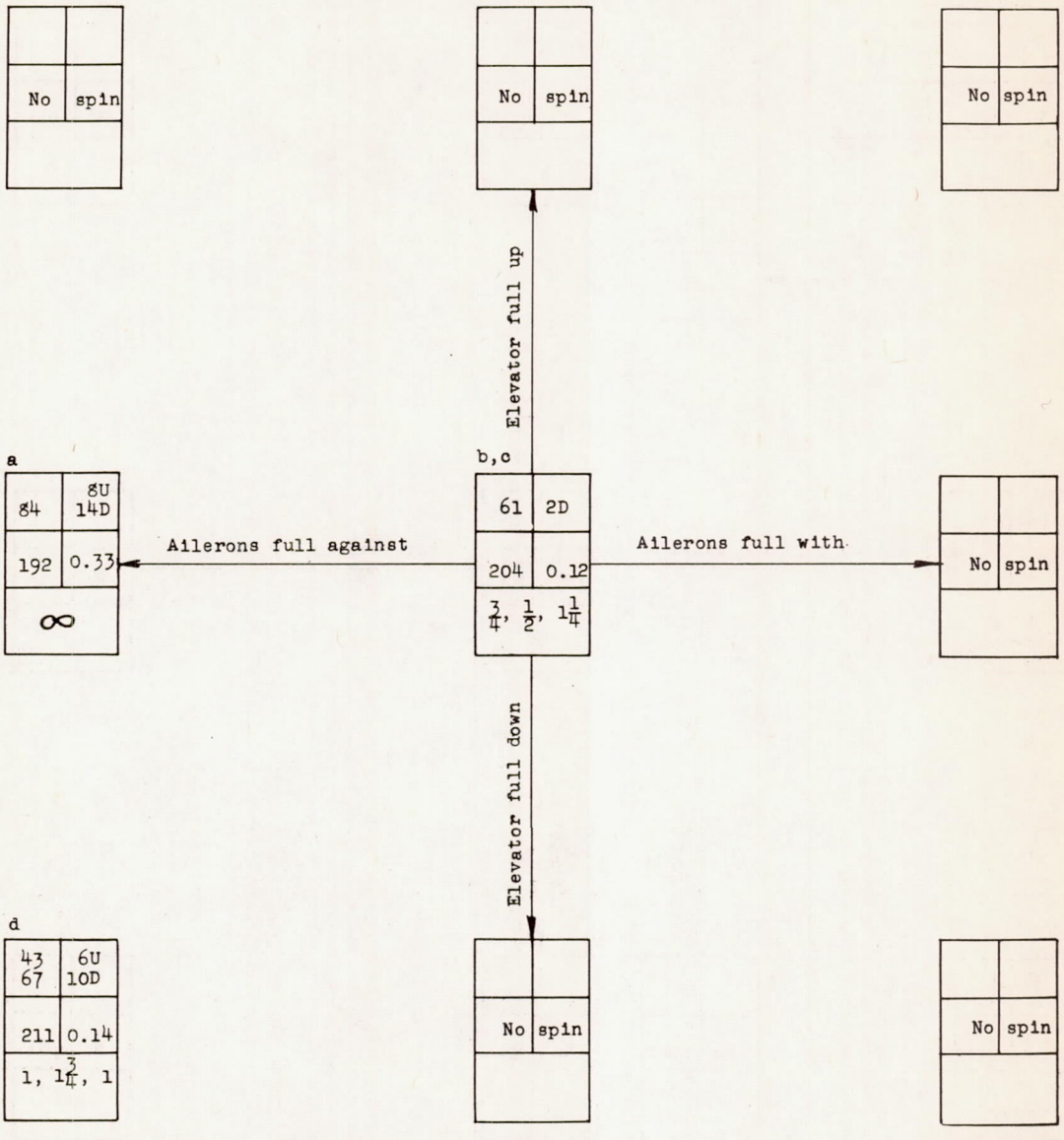
α (deg)	ϕ (deg)
V (fps)	Ω (rps)
Turns for recovery	

NACA

CHART 2(e).- SPIN CHARACTERISTICS OF MODEL FOR A LARGE RANGE OF INERTIA PARAMETERS AND RELATIVE DENSITIES; SINGLE VERTICAL TAIL INSTALLED AND CENTER OF GRAVITY AT 24 PERCENT $\bar{c}$ - Continued

$\frac{I_X - I_Y}{mb^2} = -1565 \times 10^{-4}$; $\mu = 22.60$

(Loading 9 in table III and fig. 5)



[a] Model has periodic oscillations in roll.
[b] Wide radius spin.
[c] Wandering spin.
[d] Model oscillates greatly in pitch and roll.

Model values converted to corresponding full-scale values.
U inner wing up
D inner wing down
∞ greater than 10 turns

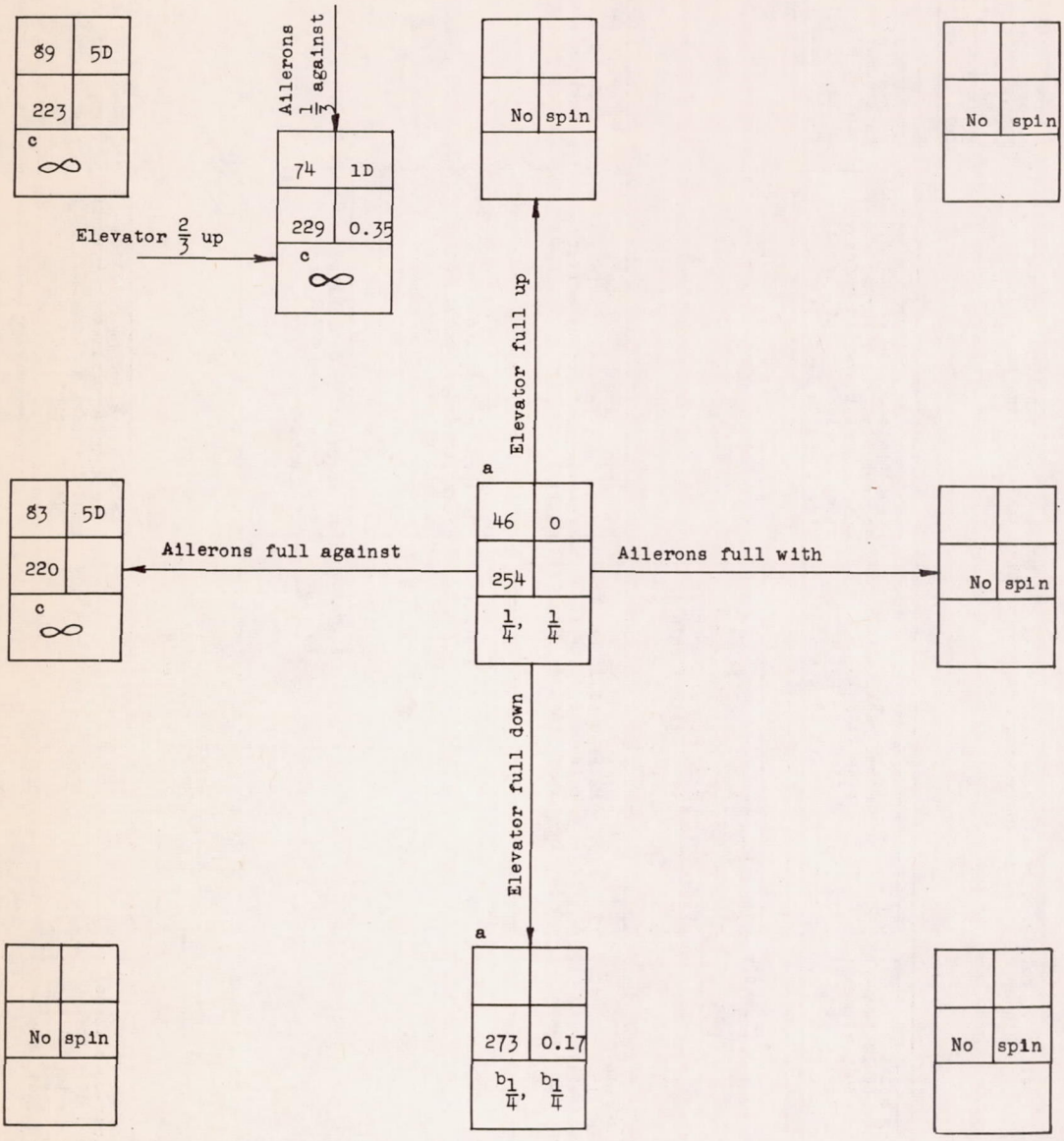
α (deg)	ϕ (deg)
V (fps)	Ω (rps)
Turns for recovery	

NACA

CHART 2(e).- SPIN CHARACTERISTICS OF MODEL FOR A LARGE RANGE OF INERTIA PARAMETERS AND RELATIVE DENSITIES; SINGLE VERTICAL TAIL INSTALLED AND CENTER OF GRAVITY AT 24 PERCENT $\bar{c}$ - Concluded

$\frac{I_X - I_Y}{mb^2} = -1431 \times 10^{-4}$; $\mu = 30.20$

(Loading 14 in table III and fig. 5)



[a] Wandering spin.

[b] After recovery from right spin, model goes into left spin.

[c] Rudder reversed from full with to 2/3 against the spin.

Model values converted to corresponding full-scale values.

U inner wing up

D inner wing down

∞ greater than 10 turns

α (deg)	φ (deg)
V (fps)	Ω (rps)
Turns for recovery	

NACA

CHART 3.- SPIN CHARACTERISTICS OF MODEL WITH THE CENTER OF GRAVITY AT 30 PERCENT $\bar{c}$; SINGLE VERTICAL TAIL INSTALLED

[Loading 15 in table III and figure 5 ($\frac{I_X - I_Y}{mb^2} = -749 \times 10^{-4}$; $\mu = 22.90$); model launched in an erect attitude with the rudder full with the direction of rotation; rotation to pilot's right. Model values converted to corresponding full-scale values. U inner wing up; D inner wing down; ∞ greater than 10 turns]

α (deg)	ϕ (deg)	Description of spin
Ω (rps)	V (fps)	
Turns for recovery by full rudder reversal		

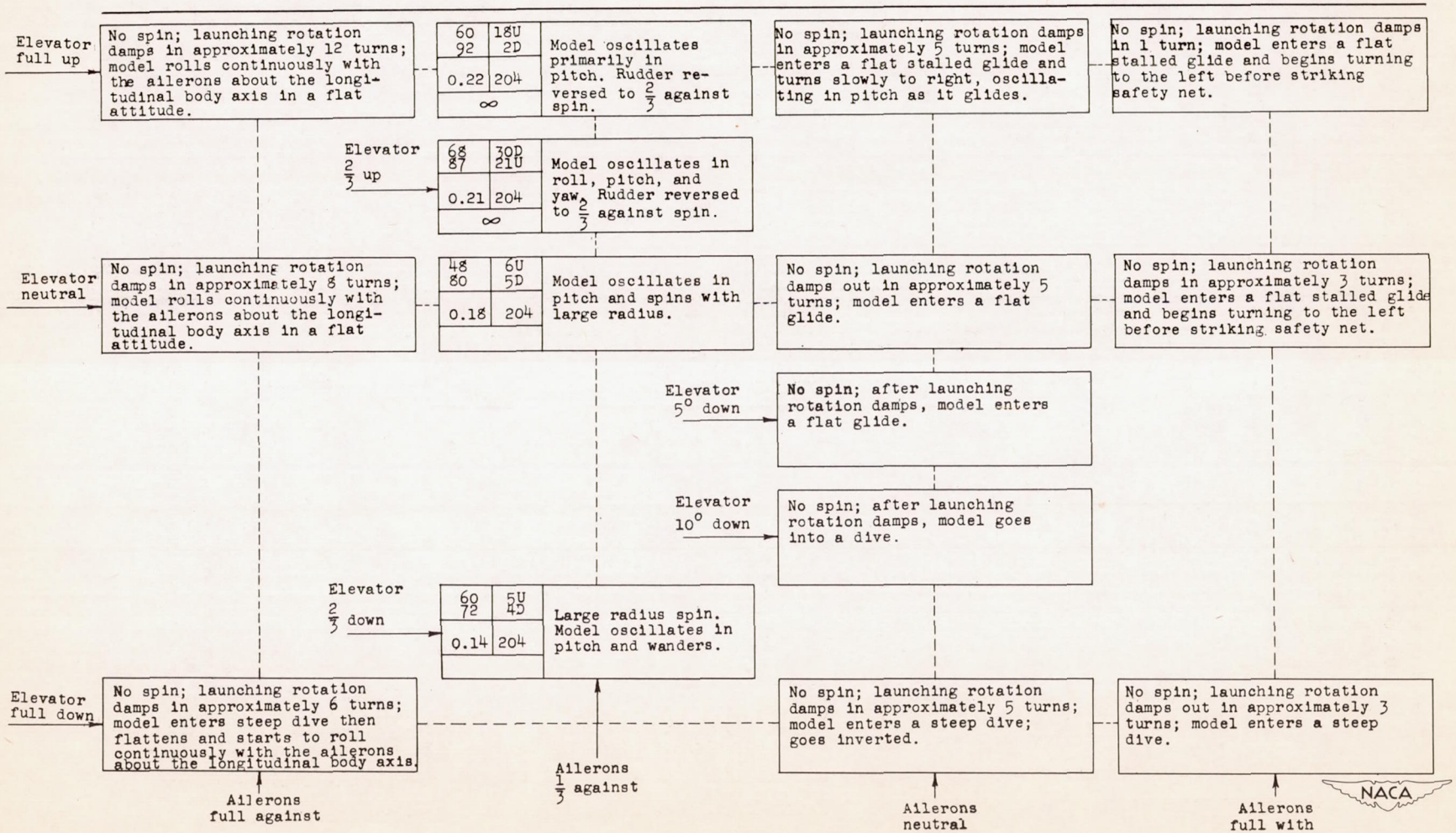


CHART 4(a).- SPIN CHARACTERISTICS OF MODEL WITH CENTER OF GRAVITY AT 35 PERCENT $\bar{c}$; SINGLE VERTICAL TAIL INSTALLED

[Loading 16 in table III and figure 5 ($\frac{I_X - I_Y}{mb^2} = -697 \times 10^{-4}$; $\mu = 22.90$); model launched in an erect attitude with the rudder full with the direction of rotation; recovery attempted by reversing the rudder from full with to full against the spin unless otherwise noted; rotation to pilot's right. Model values converted to corresponding full-scale values. U inner wing up; D inner wing down; ∞ greater than 10 turns]

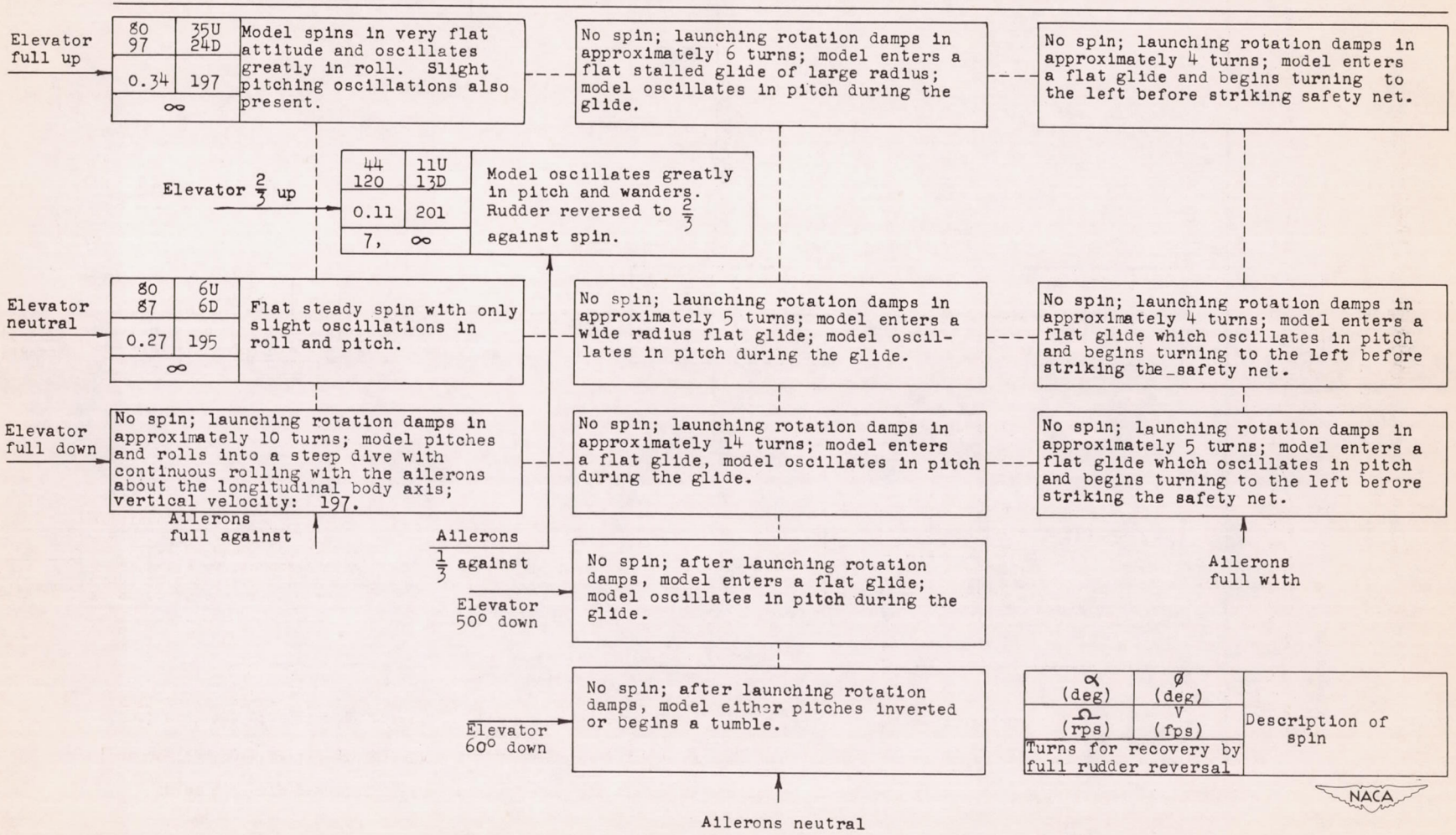
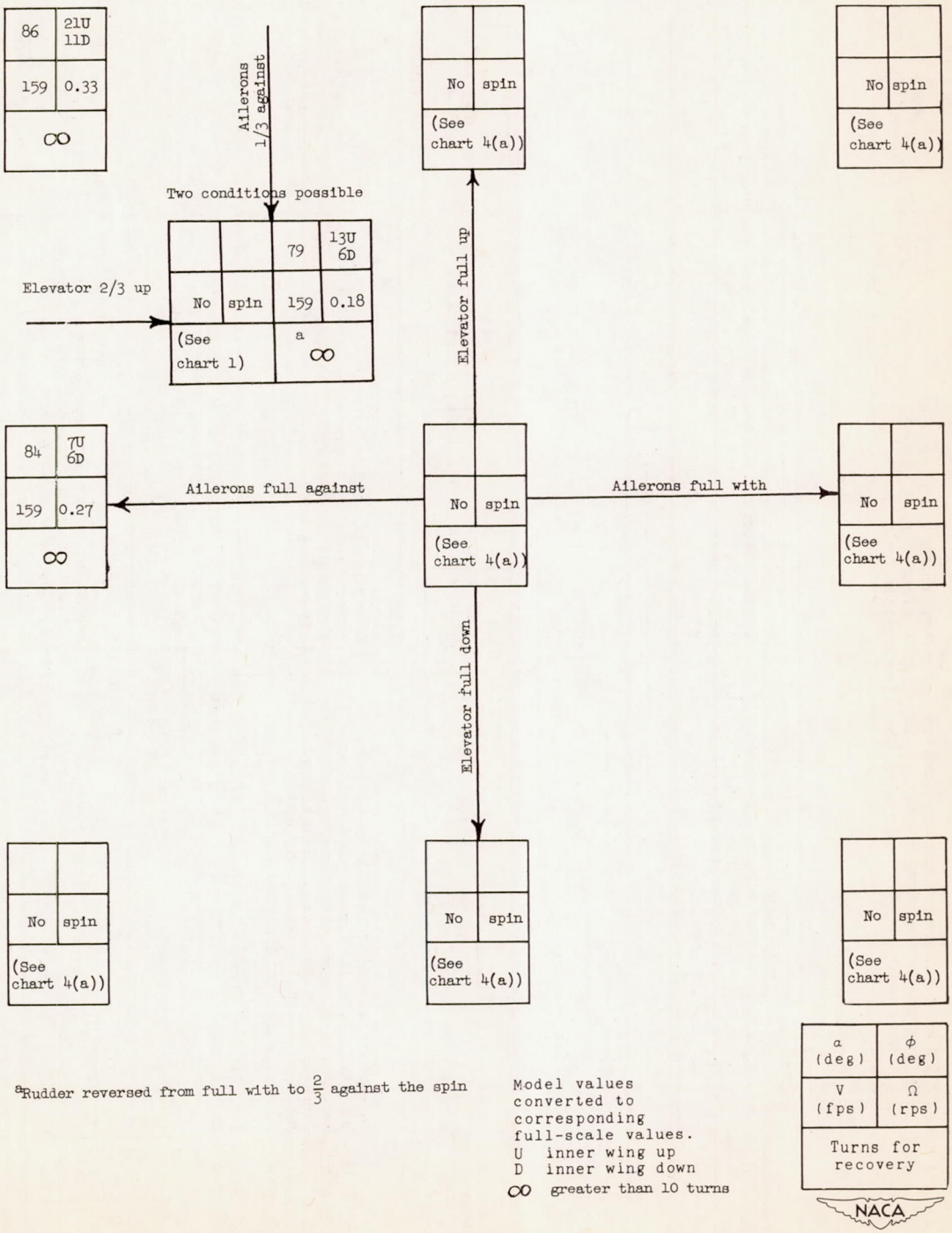


CHART 4b.— SPIN CHARACTERISTICS OF MODEL WITH CENTER OF GRAVITY AT 35 PERCENT $\bar{c}$;

SINGLE VERTICAL TAIL INSTALLED

[Loading 17 in table III and figure 5 $\left(\frac{I_X - I_Y}{mb^2} = -1442 \times 10^{-4}; \mu = 15.00\right)$; model launched in an erect attitude with the rudder full with the direction of rotation; recoveries attempted by reversing the rudder from full with to full against the spin unless otherwise noted; rotation to pilot's right]



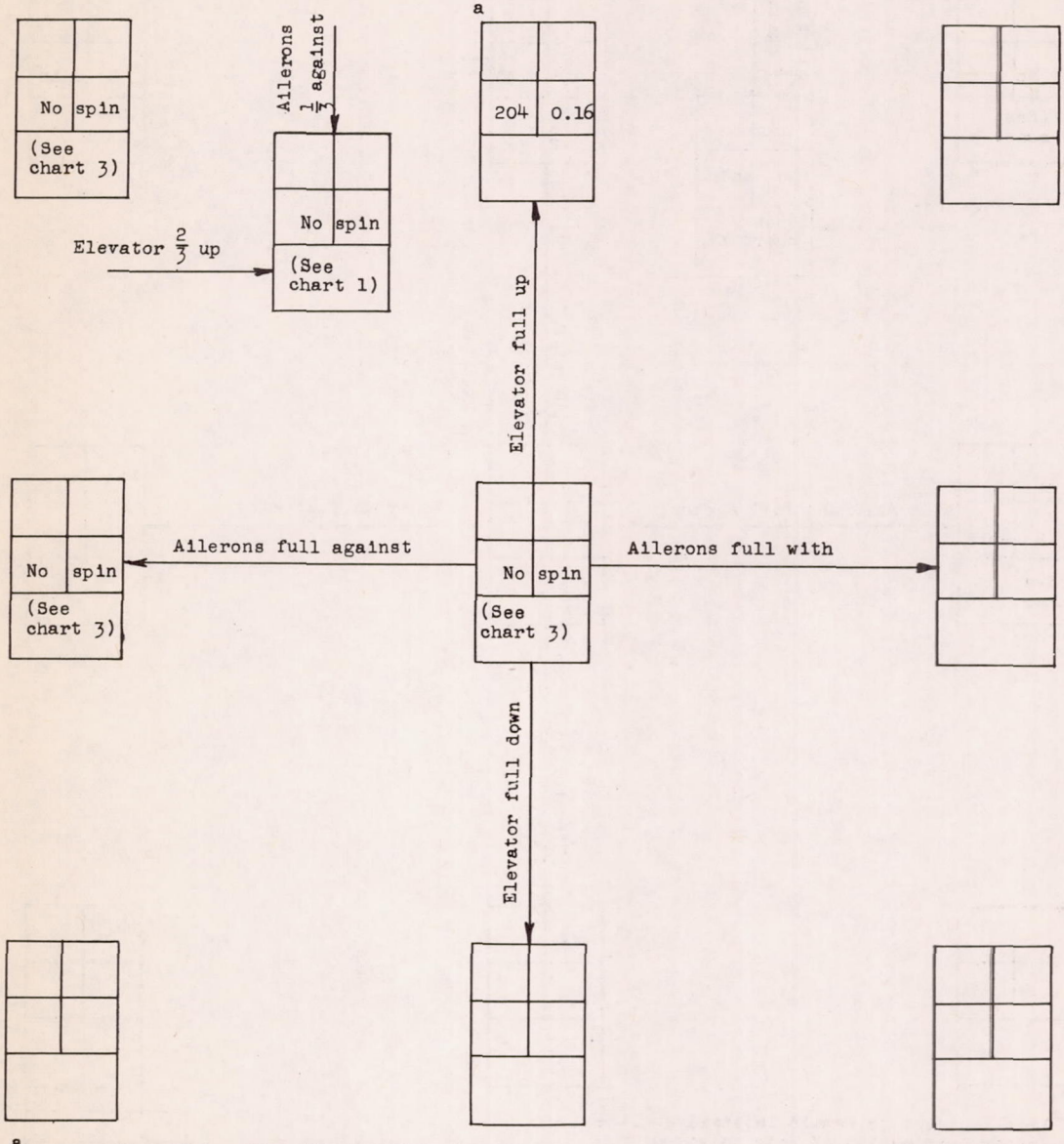
[a]Rudder reversed from full with to $\frac{2}{3}$ against the spin

Model values converted to corresponding full-scale values.
U inner wing up
D inner wing down
∞ greater than 10 turns

CHART 5.- SPIN CHARACTERISTICS OF MODEL WITH VARIOUS VERTICAL TAIL ARRANGEMENTS INSTALLED; CENTER OF GRAVITY AT 30 PERCENT $\bar{c}$

[Loading number 15 on table III and fig. 5 ($\frac{I_X - I_Y}{mb^2} = -749 \times 10^{-4}$; $\mu = 22.90$); tail arrangement as indicated; model launched in an erect attitude with the rudders fixed full with the direction of rotation; recoveries attempted by reversing the rudders from full with to full against the spin unless otherwise noted; rotation to pilot's right]

Small dual and single vertical tail installed (fig. 2)



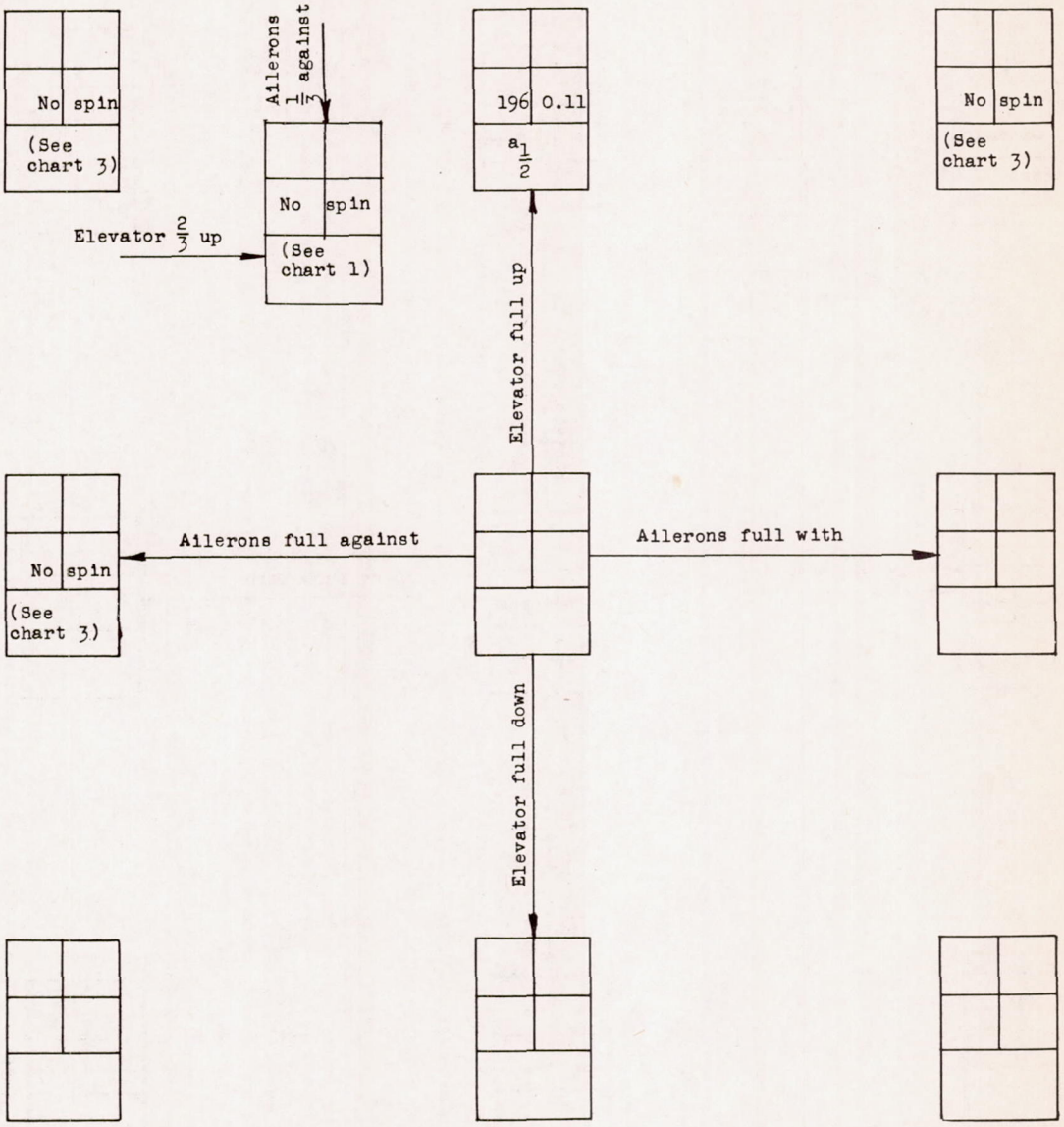
[a]Large radius flat spin. Termination of spin rotation indicated to be rapid from this spin by reversal of rudders inasmuch as forced spin rotation damped rapidly when model was launched with the rudders set against spin.

Model values converted to corresponding full-scale values.
U inner wing up
D inner wing down

NACA

CHART 5.- SPIN CHARACTERISTICS OF MODEL WITH VARIOUS TAIL ARRANGEMENTS INSTALLED; CENTER OF GRAVITY AT 30 PERCENT $\bar{c}$ - Continued

Medium size dual vertical tails installed (fig. 2)

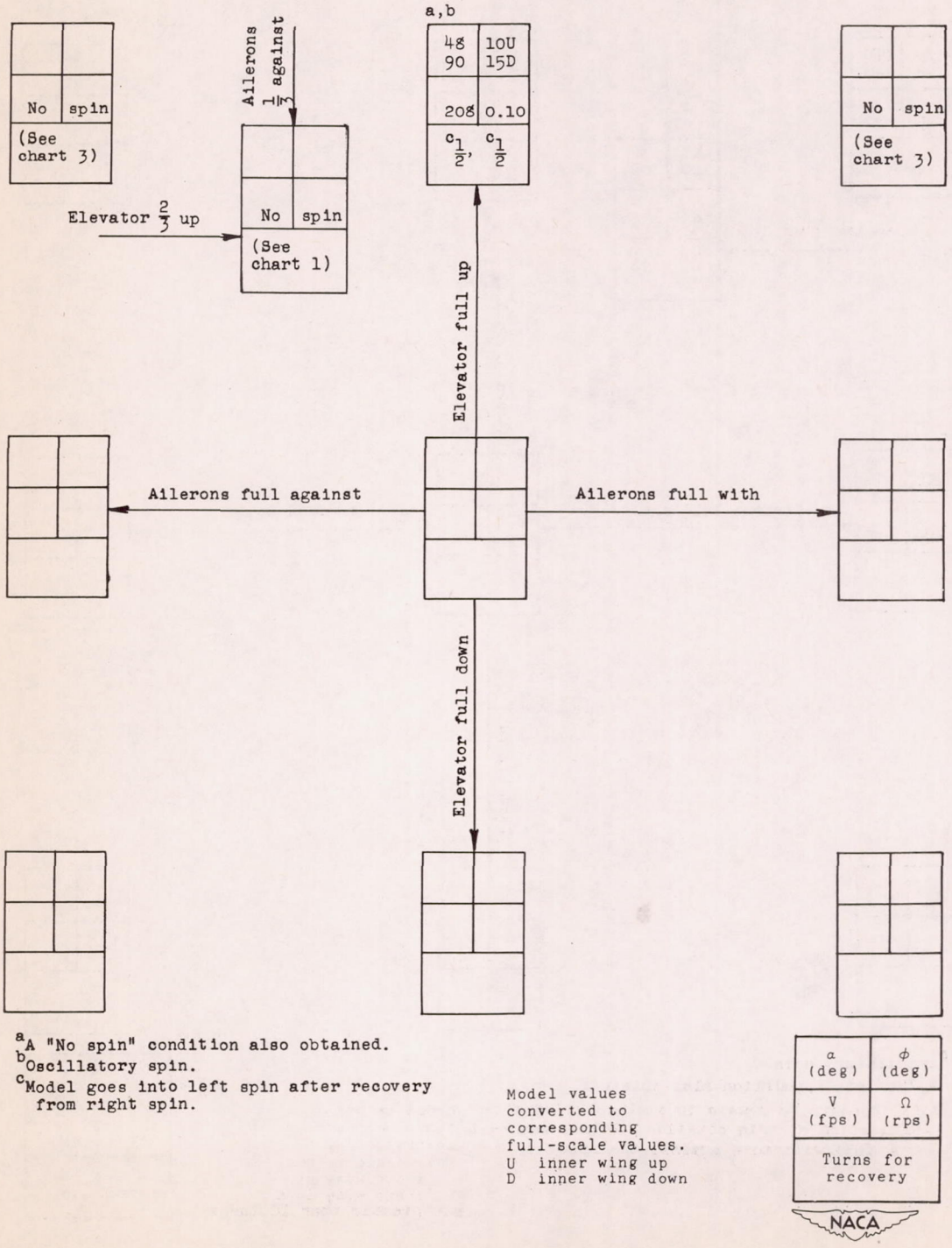


[a]Model appears to remain in stalled glide after termination of spin rotation.

Model values converted to corresponding full-scale values
U inner wing up
D inner wing down

CHART 5.- SPIN CHARACTERISTICS OF MODEL WITH VARIOUS VERTICAL TAIL ARRANGEMENTS INSTALLED; CENTER OF GRAVITY AT 30 PERCENT $\bar{c}$ - Concluded

Large size dual vertical tails installed (fig. 2)



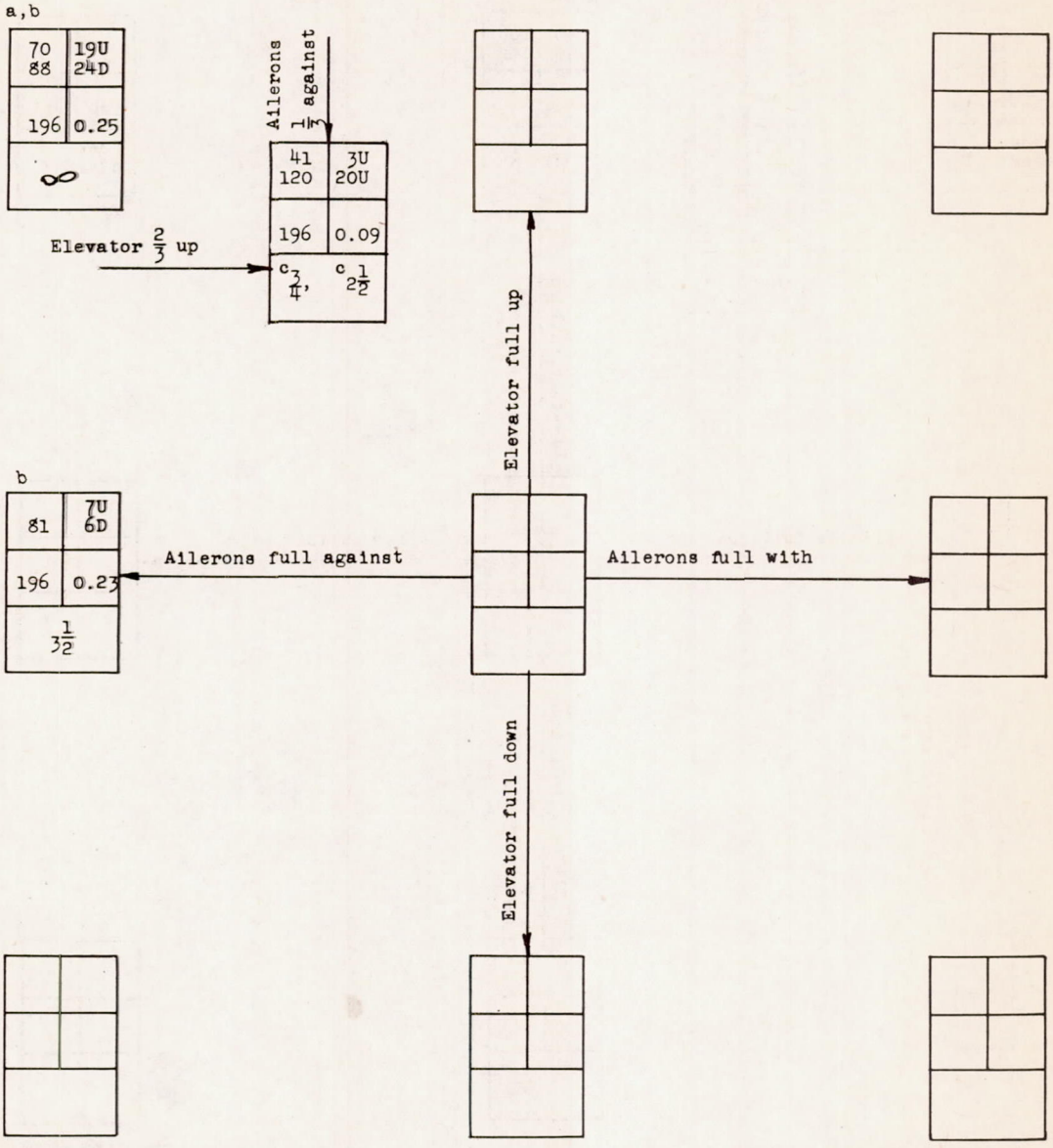
[a]A "No spin" condition also obtained.
[b]Oscillatory spin.
[c]Model goes into left spin after recovery from right spin.

Model values converted to corresponding full-scale values.
U inner wing up
D inner wing down

CHART 6.- SPIN CHARACTERISTICS OF MODEL WITH VARIOUS VERTICAL TAIL ARRANGEMENTS INSTALLED; CENTER OF GRAVITY AT 35 PERCENT $\bar{c}$

[Loading number 16 on table III and fig. 5 ($\frac{I_X - I_Y}{mb^2}$ = -697 x 10^{-4}; μ = 22.90); tail arrangement as indicated; model launched in an erect attitude with the rudders fixed full with the direction of rotation; recoveries attempted by reversing the rudders from full with to full against the spin unless otherwise noted; rotation to pilot's right]

Small dual and single vertical tail installed (fig. 2)



[a] Oscillatory spin.

[b] A "No spin" condition also obtained.

[c] Model appears to remain in stalled glide after termination of spin rotation. Rudder reversed from full with to 2/3 against the spin.

Model values converted to corresponding full-scale values.

U inner wing up

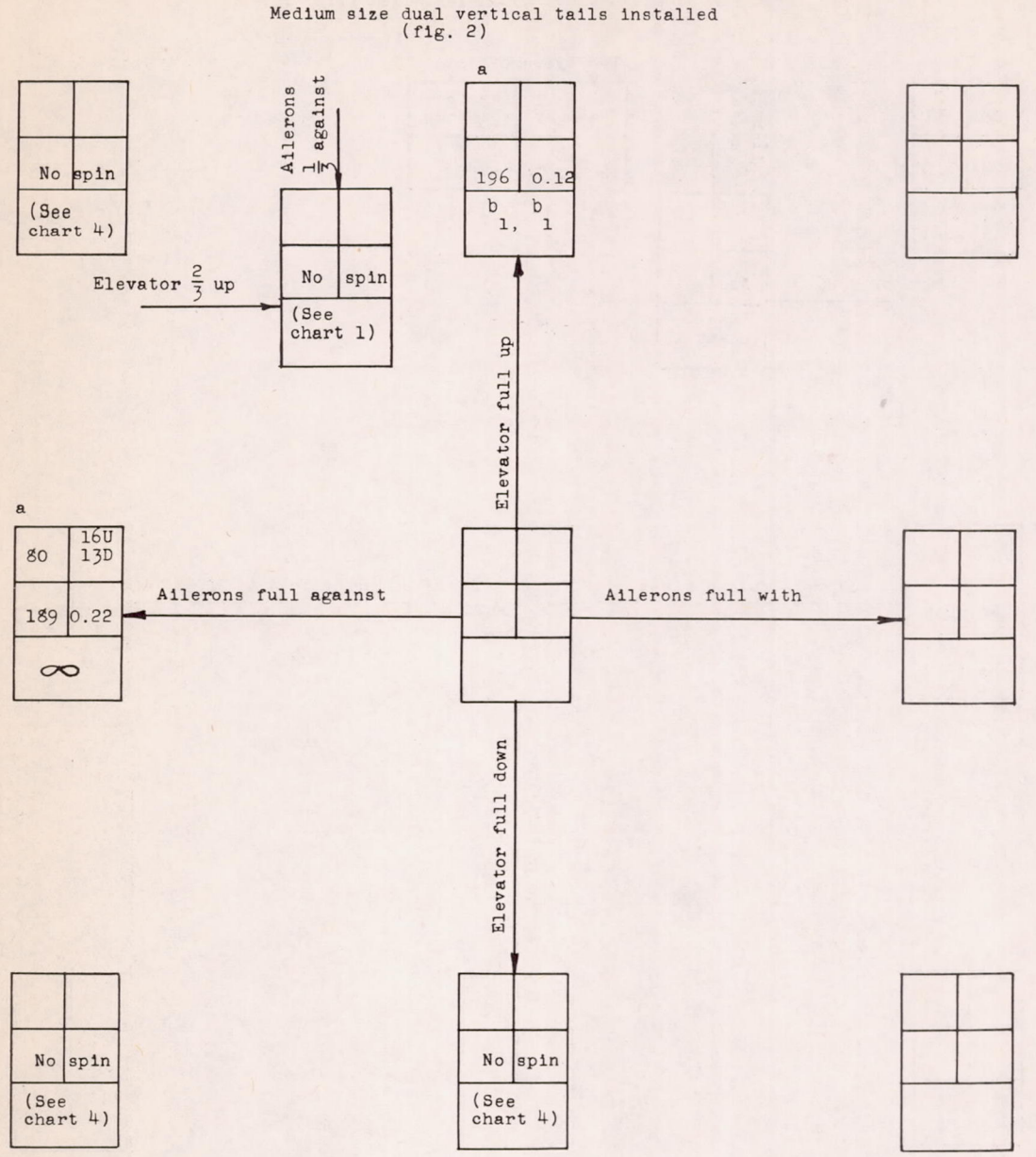
D inner wing down

∞ greater than 10 turns

α (deg)	ϕ (deg)
V (fps)	Ω (rps)
Turns for recovery	

NACA

CHART 6.- SPIN CHARACTERISTICS OF MODEL WITH VARIOUS VERTICAL TAIL ARRANGEMENTS INSTALLED; CENTER OF GRAVITY AT 35 PERCENT $\bar{c}$ - Continued



[a] A "No spin" condition also obtained.

[b] Model appears to remain in stalled glide after termination of spin rotation.

Model values converted to corresponding full-scale values.

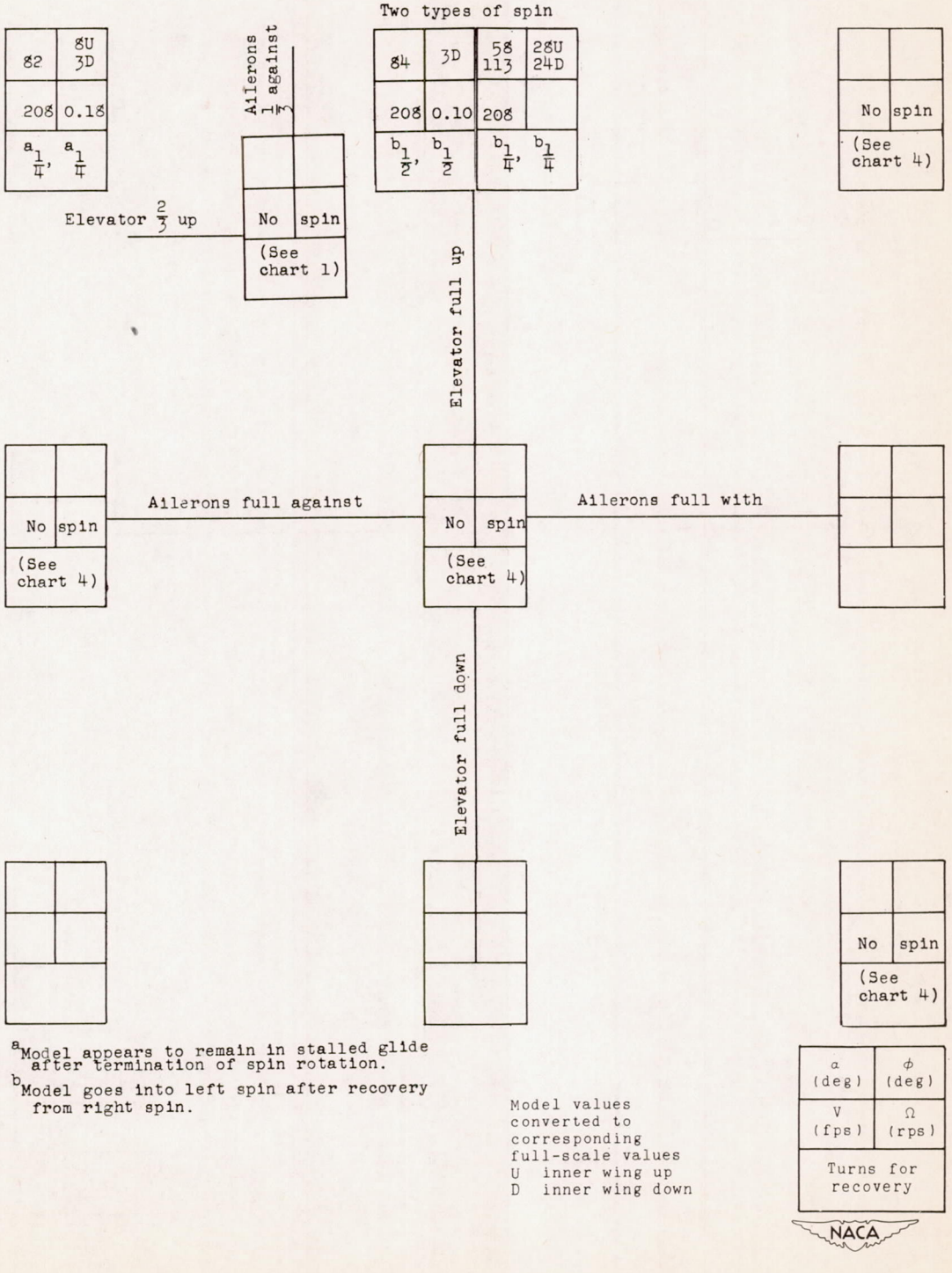
U inner wing up

D inner wing down

∞ greater than 10 turns

CHART 6.- SPIN CHARACTERISTICS OF MODEL WITH VARIOUS VERTICAL TAIL ARRANGEMENTS INSTALLED; CENTER OF GRAVITY AT 35 PERCENT $\bar{c}$ - Concluded

Large size dual vertical tails installed (fig. 2)



[a] Model appears to remain in stalled glide after termination of spin rotation.

[b] Model goes into left spin after recovery from right spin.

Model values converted to corresponding full-scale values
U inner wing up
D inner wing down

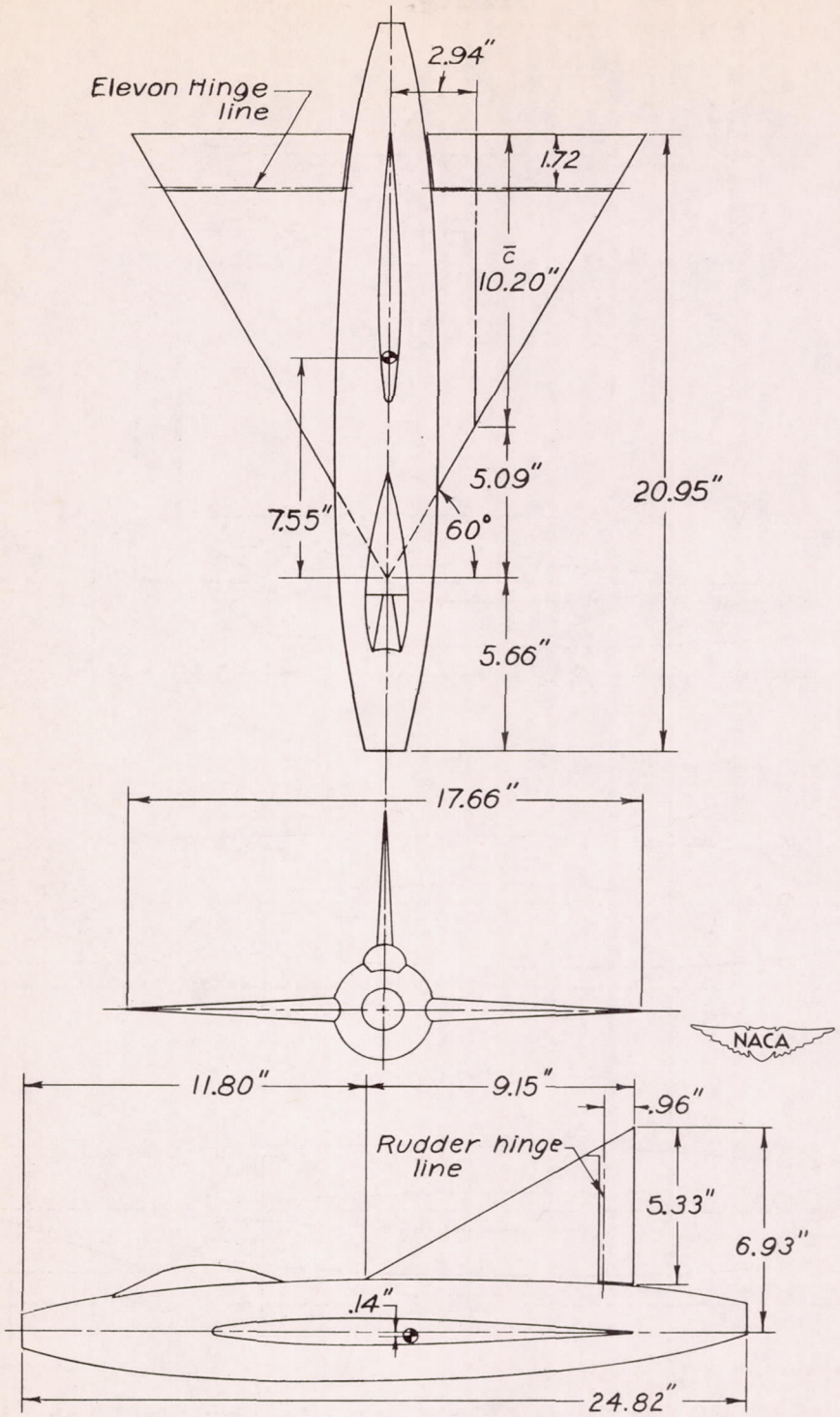


Figure 1.- Drawing of the $\frac{1}{20}$-scale model tested in the Langley 20-foot free-spinning tunnel. Center of gravity positioned at 24 percent $\bar{c}$.

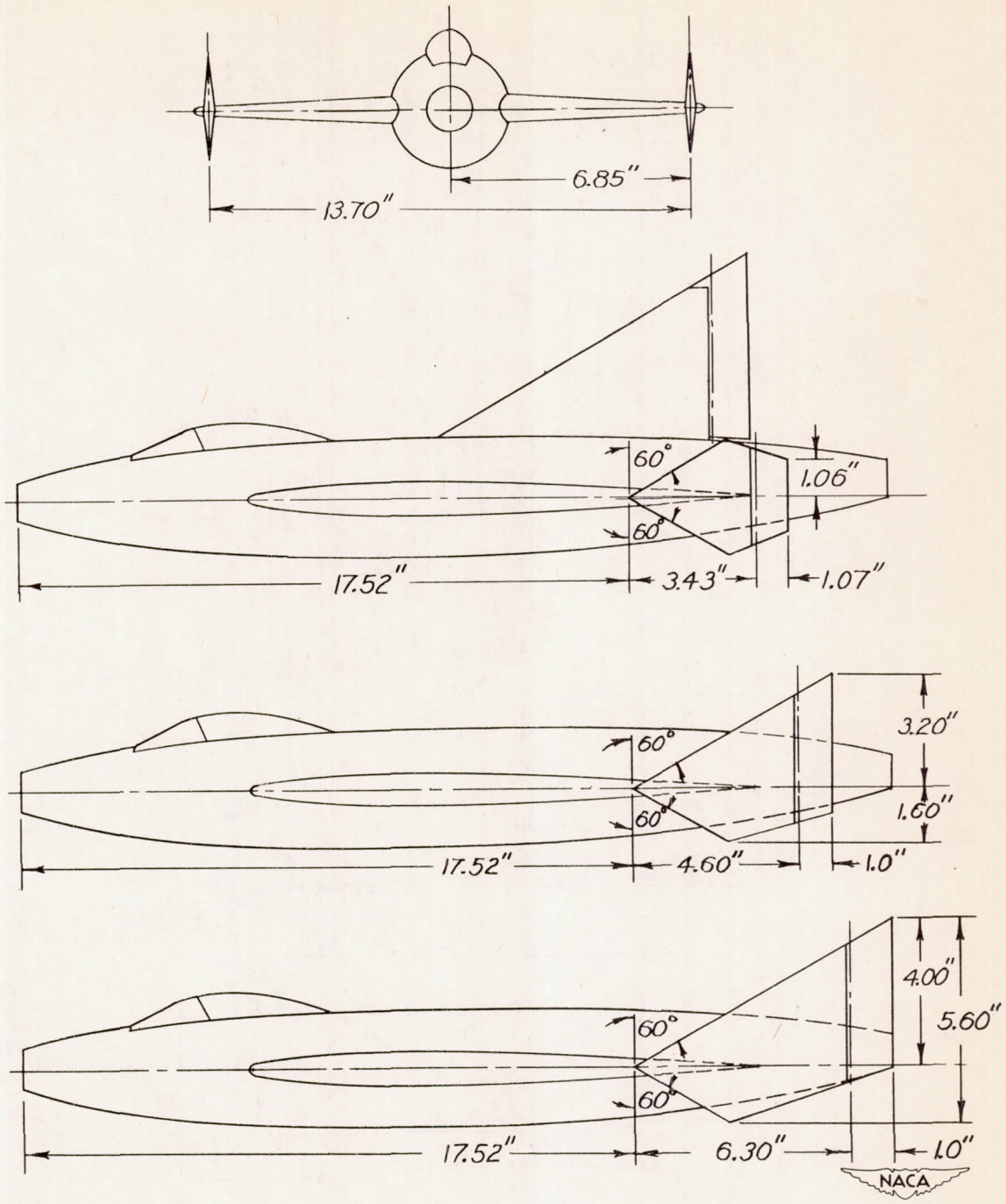


Figure 2.- Comparison of the various vertical-multitail arrangements tested on the $\frac{1}{20}$-scale model (values are model dimensions).

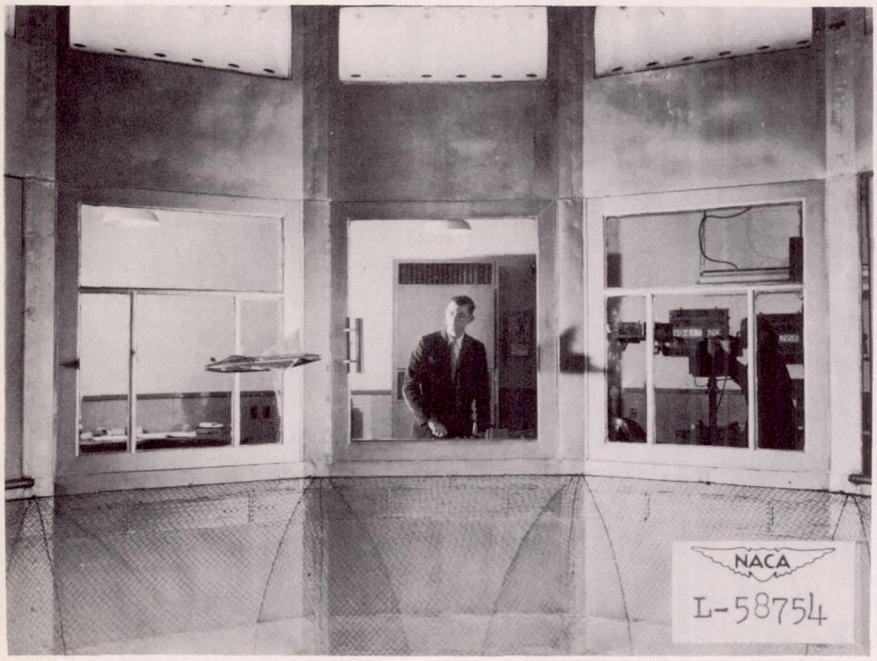


Figure 3.- Photograph of the $\frac{1}{20}$-scale model spinning in the Langley 20-foot free-spinning tunnel.

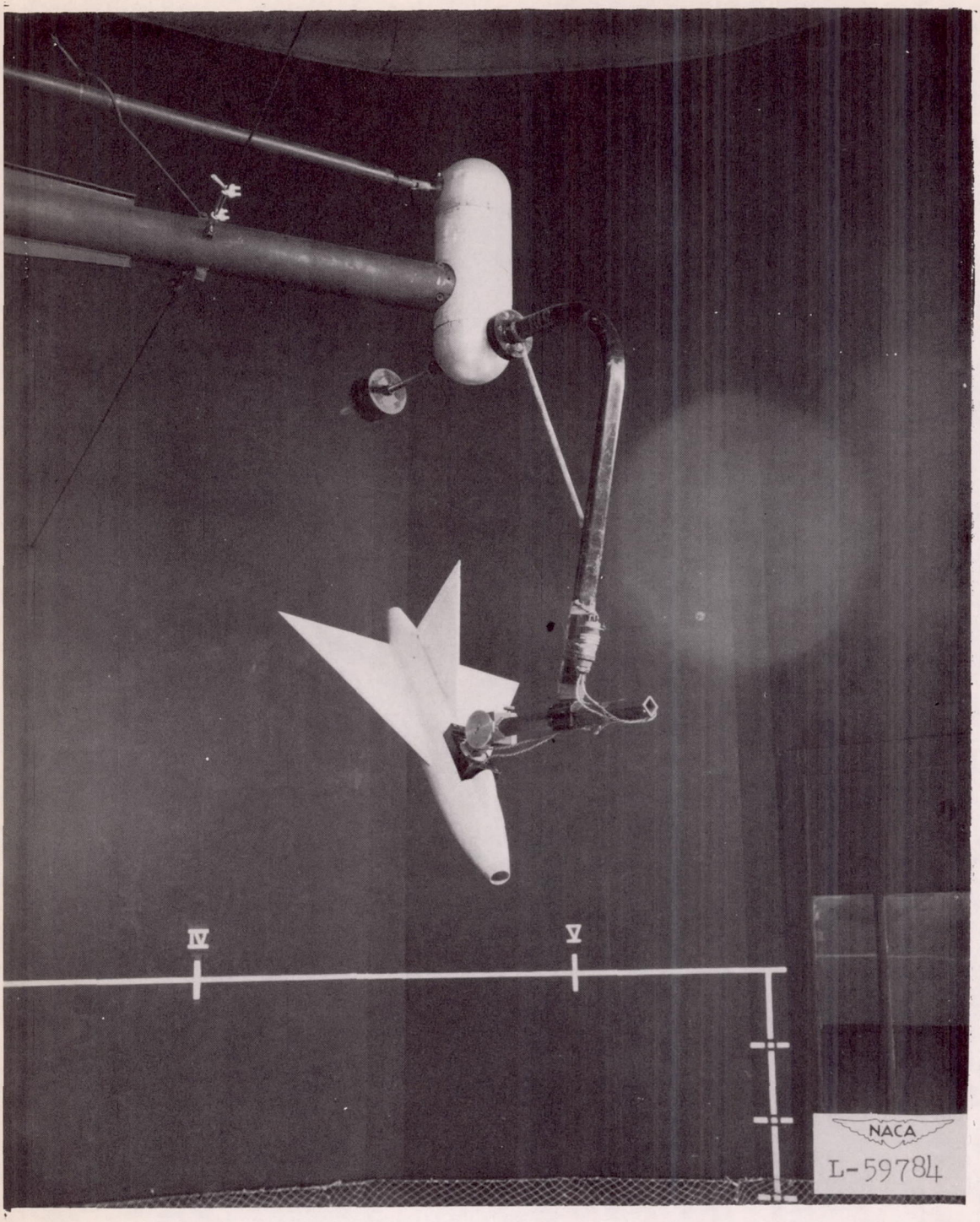


Figure 4.- Photograph of the $\frac{1}{12}$-scale model mounted on the strain-gage balance in the Langley 20-foot free-spinning tunnel.

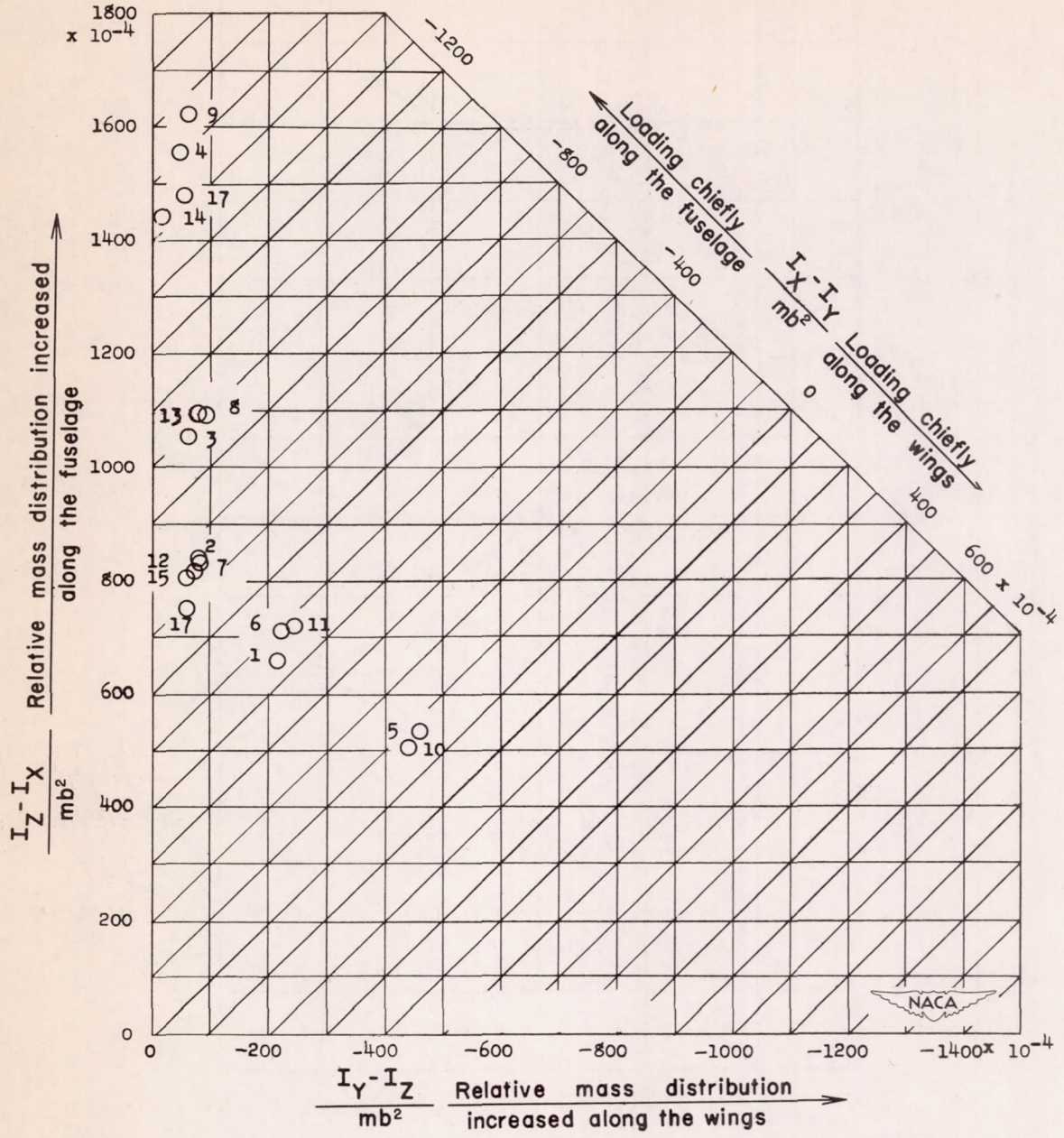


Figure 5.– Inertia parameters for loadings tested on the $\frac{1}{20}$–scale model. (Points are for loadings listed in table III.)

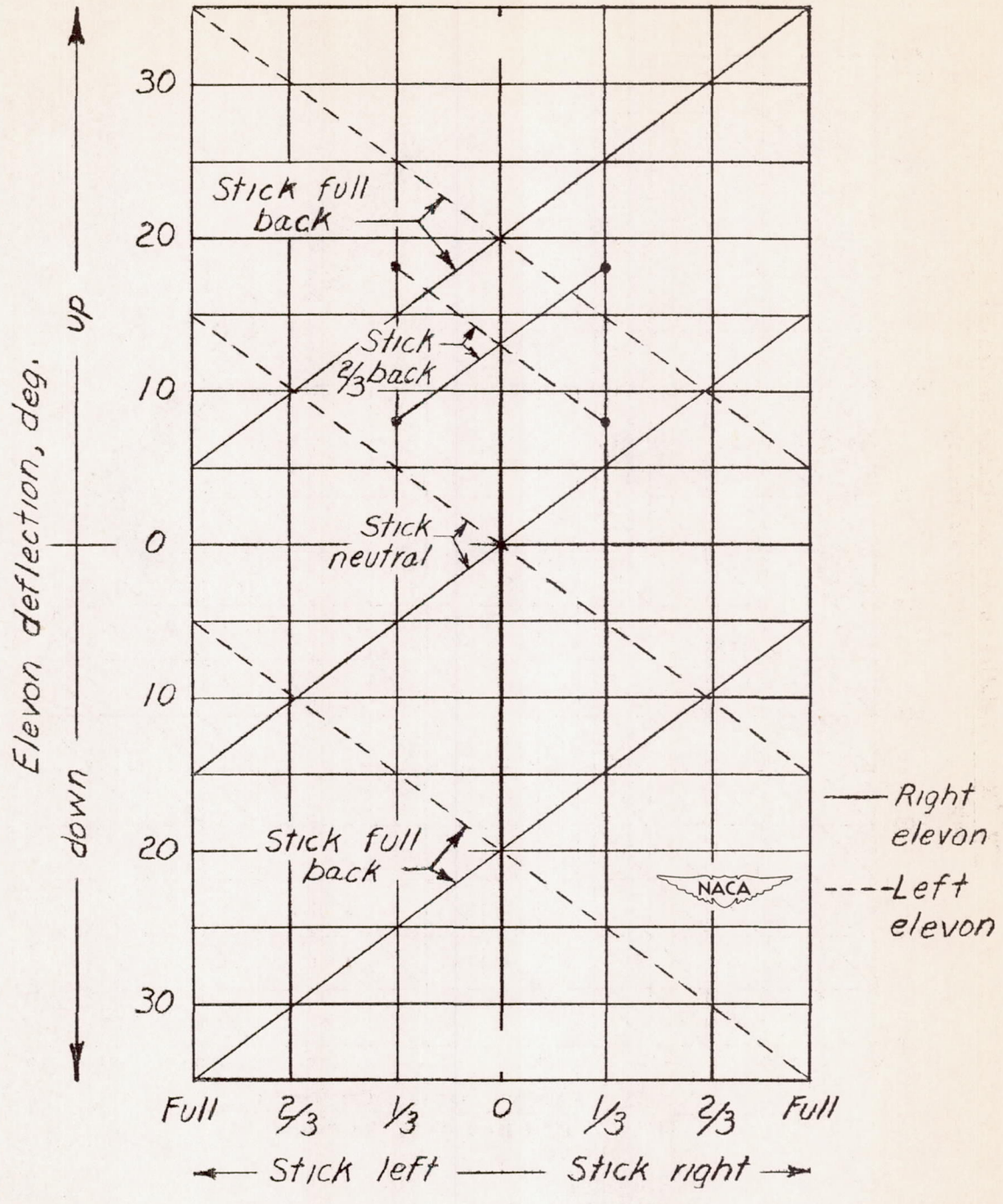


Figure 6.- Elevon deflections used on the models for various control-stick positions.

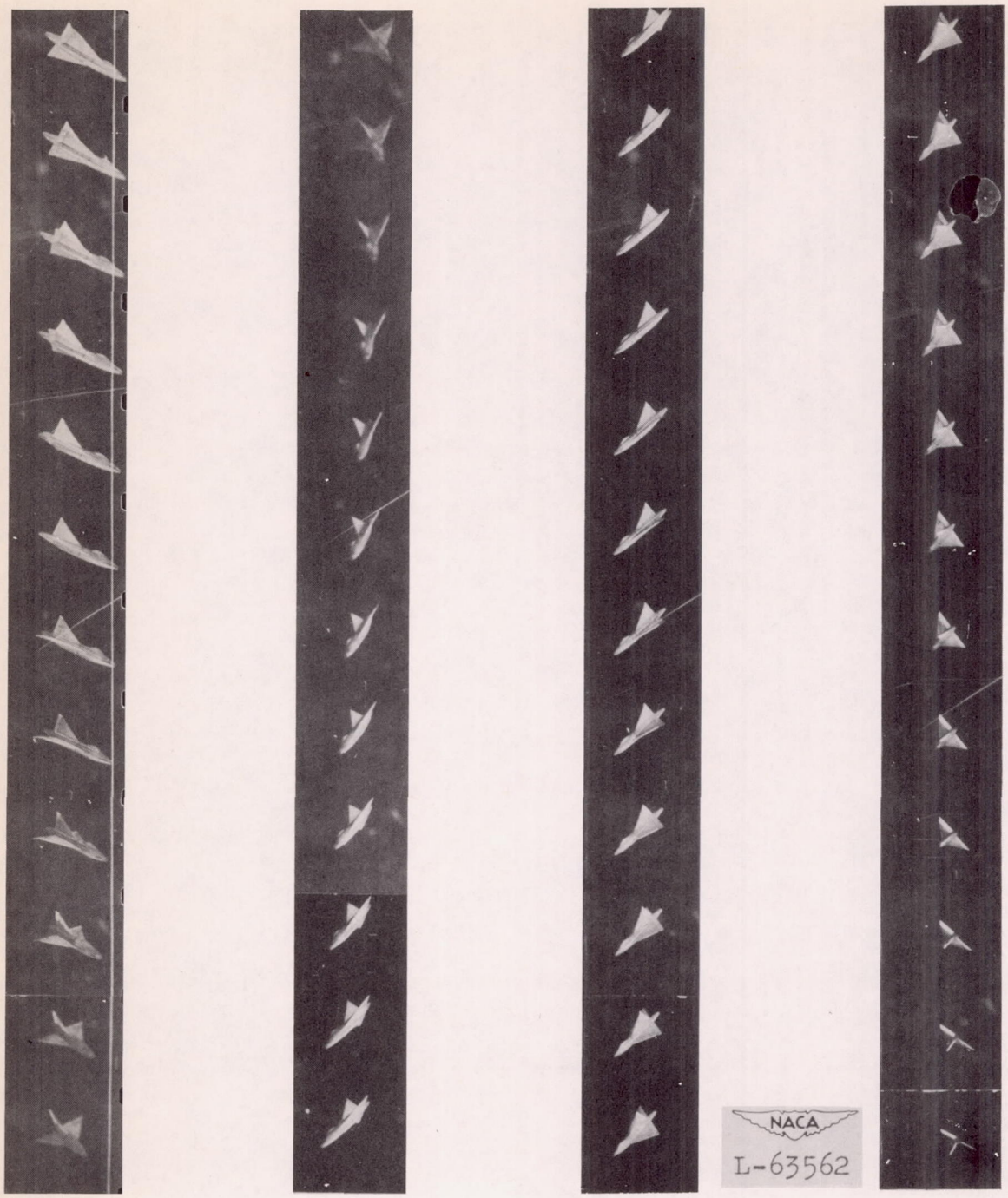


Figure 7.– Typical rolling motion of the $\frac{1}{20}$–scale model with ailerons set against the spin following launching with spinning rotation. The center of gravity is at 24 percent $\bar{c}$. Camera speed is 64 frames per second.

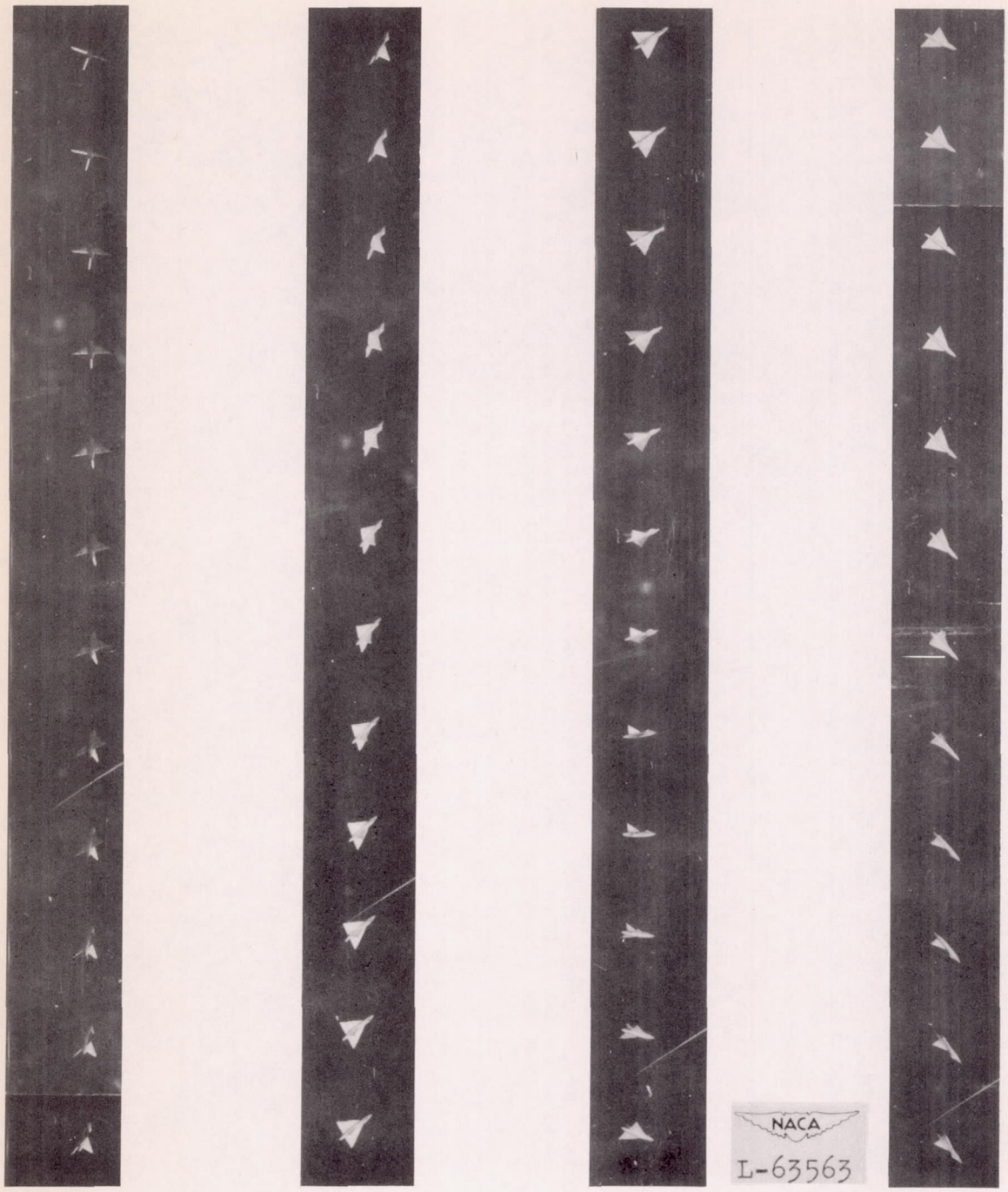


Figure 7.- Continued.

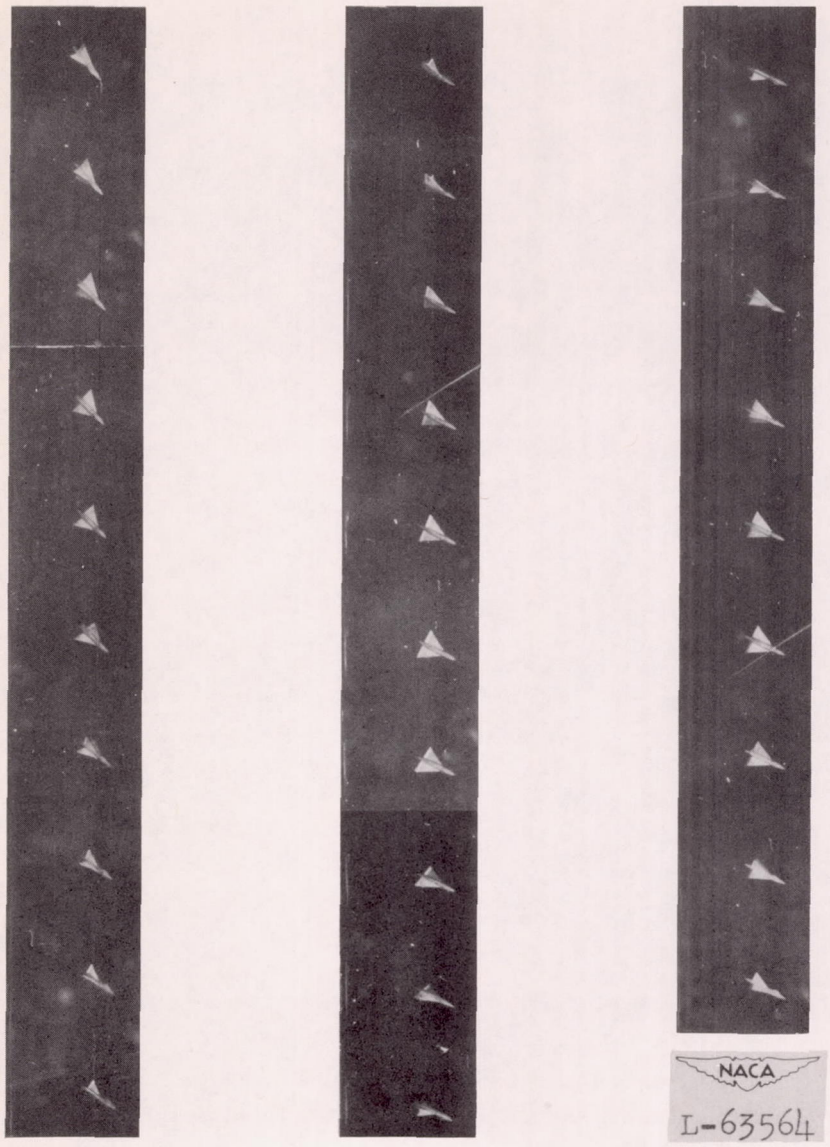


Figure 7.- Concluded.

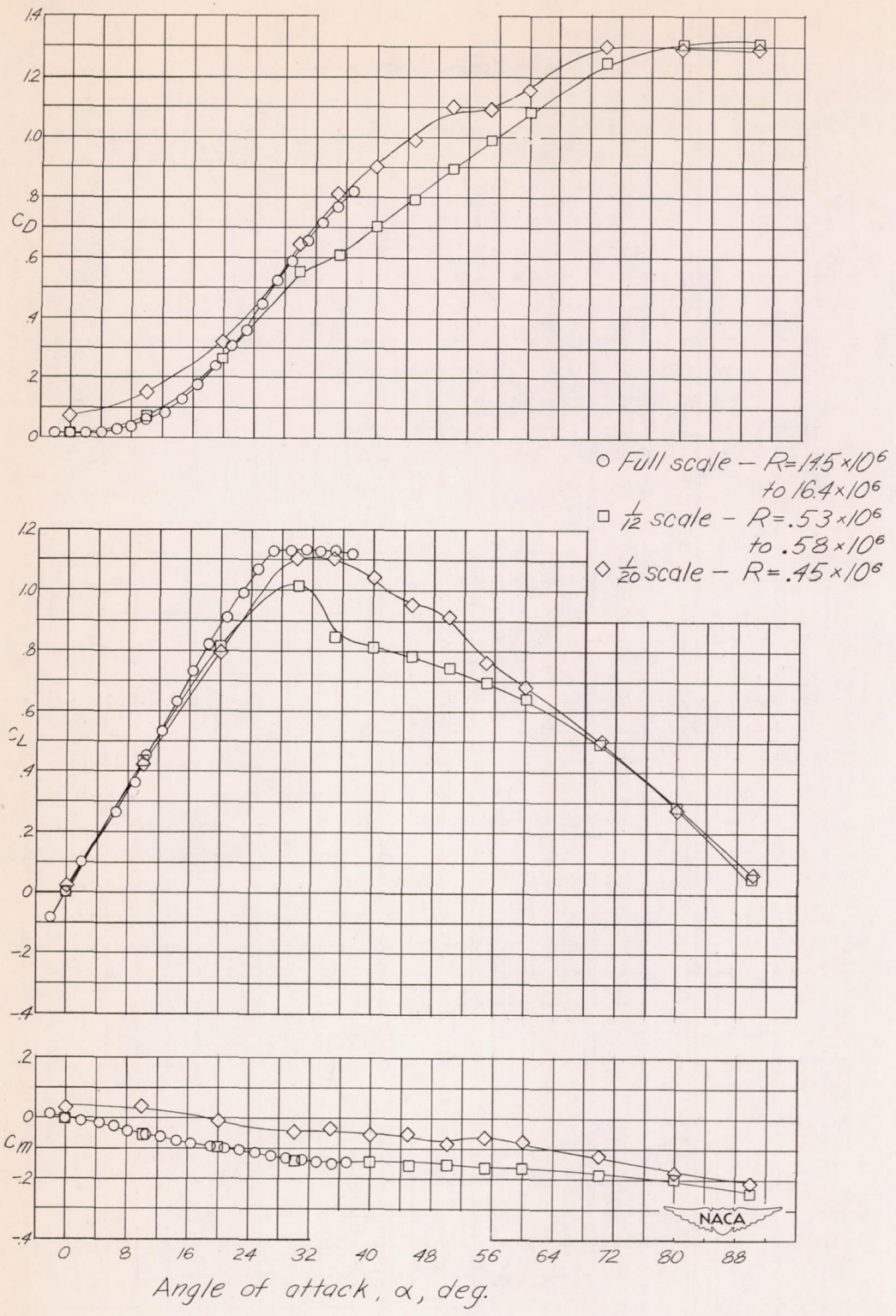


Figure 8.– Comparison of the aerodynamic characteristics in pitch of the $\frac{1}{20}$ – and $\frac{1}{12}$ –scale models and a similar full-scale airplane. Center of gravity at 24 percent $\bar{c}$. $\Psi = 0^\circ$, $\delta_e = 0^\circ$, $\delta_a = 0^\circ$, $\delta_r = 0^\circ$.

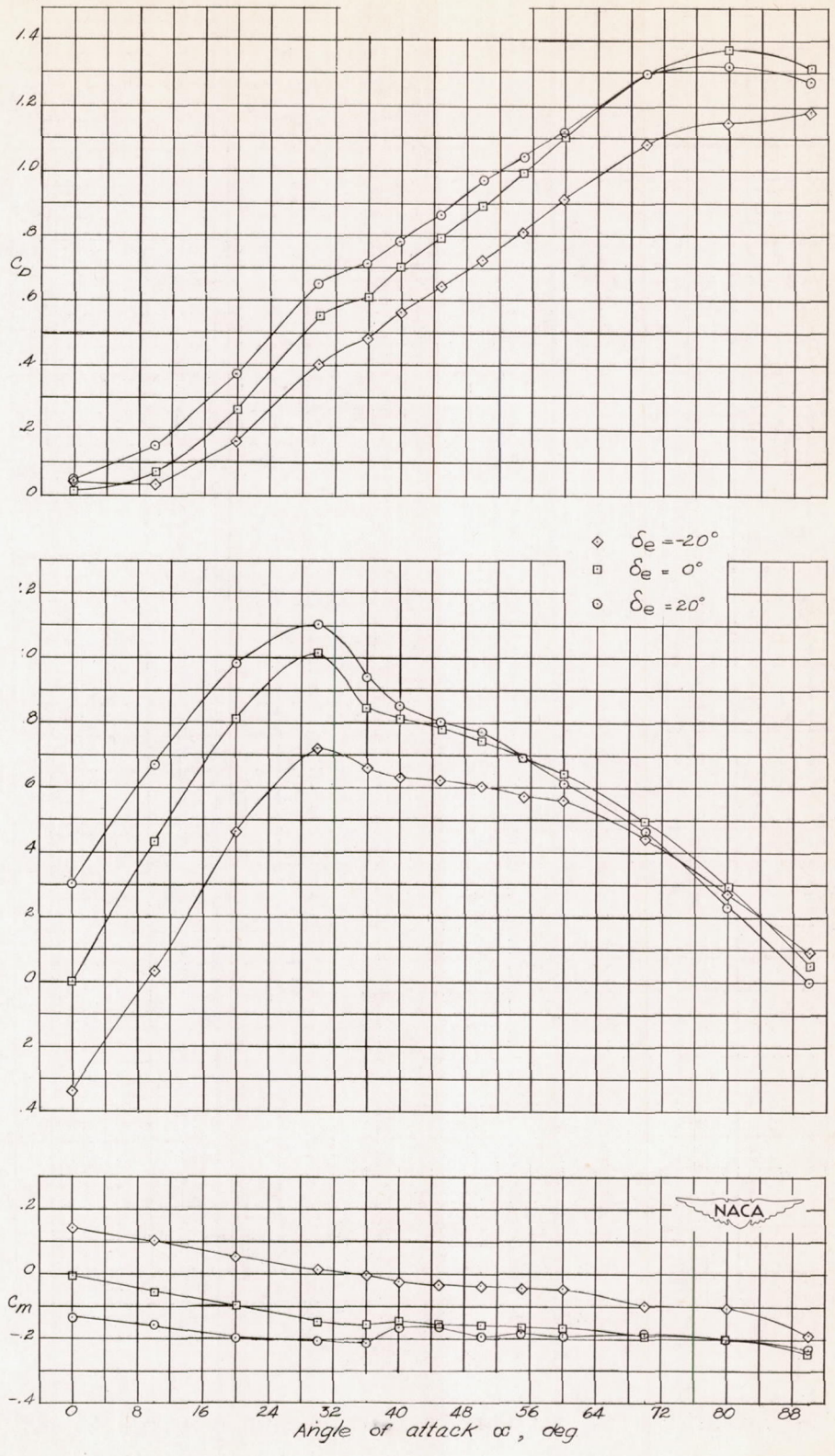


Figure 9.– Aerodynamic characteristics in pitch of the $\frac{1}{12}$-scale model. Center of gravity at 24 percent $\bar{c}$. $\psi = 0°$, $\delta_r = 0°$, $\delta_a = 0°$.